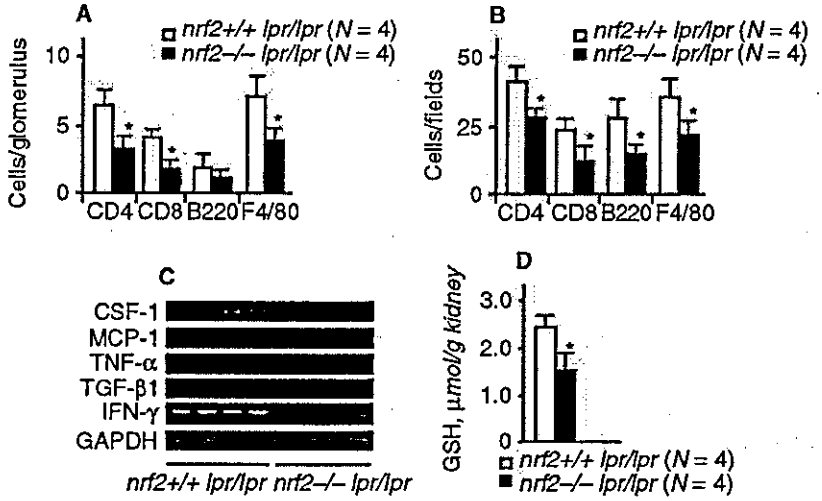

Fig. 3. Renal profile of infiltrated leukocytes and macrophages, key cytokines, and glutathione (GSH) levels. The numbers of macrophage (F4/80), CD4, CD8-positive T cells, and B220 positive cells were significantly reduced in the glomeruli and interstitium of *nrf2−/− lpr/lpr* kidneys compared with *nrf2+/+ lpr/lpr* kidneys in immunohistochemical examination (*A* and *B*). Colony stimulating factor 1 (CSF-1), monocyte chemoattractant protein 1 (MCP-1), tumor necrosis factor-α (TNF-α), transforming growth factor-β1 (TGF-β1), and interferon γ (IFN-γ) levels were reduced in *nrf2−/− lpr/lpr* kidneys compared to *nrf2+/+ lpr/lpr* kidneys [reverse transcription-polymerase chain reaction (RT-PCR) method] (*C*). Renal GSH was significantly reduced in *nrf2−/− lpr/lpr* mice compared to *nrf2+/+ lpr/lpr* mice (*D*). Each bar represents the mean ± SEM. $^*P < 0.05$.

at 100 units, the titer of anti-double-stranded DNA autoantibody in *nrf2+/+ lpr/lpr* female mice was equal to MRL/*lpr* female mice.

Lymphadenopathy scoring

MRL/*lpr* mice develop massive lymphadenopathy due to a defect in Fas [16]. Therefore, lymphadenopathy in *nrf2−/− lpr/lpr* mice was evaluated. The scoring of lymphadenopathy was assigned by an observer, as described in the **Methods** section. The average score value was decreased in *nrf2−/− lpr/lpr* mice (Table 1).

FACS analysis of lymph nodes

We found lymphadenopathy was improved in *nrf2−/− lpr/lpr* mice. Next, we performed FACS analysis to examine the subset of lymphocytes and macrophages in lymph nodes. The numbers of CD4, CD8-positive, double-negative T cells and macrophage (F4/80) was significantly reduced in *nrf2−/− lpr/lpr* lymph nodes compared with *nrf2+/+ lpr/lpr* lymph nodes (Fig. 4).

TUNEL assay of spleen and kidney

Since Fas-mediated apoptosis is defective in *lpr* mice, the immunologic improvements seen in *nrf2−/− lpr/lpr* mice suggested that the activity of Nrf2 might somehow be linked to Fas-mediated apoptosis. Therefore, apoptosis in spleen and kidney was examined. The indices of TUNEL-positive cells were significantly increased in *nrf2−/− lpr/lpr* mice compared to *nrf2+/+ lpr/lpr* mice (Fig. 5). We observed apoptosis was increased in *nrf2−/− lpr/lpr* spleens and kidneys.

Induction of TNF-α–mediated apoptosis in splenocytes

We examined the effect of apoptosis triggered by anti-Fas antibody in splenocytes obtained from *nrf2−/−*

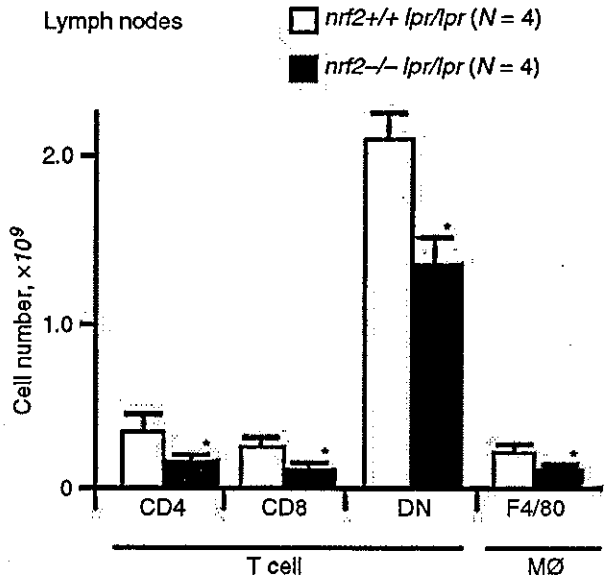

Fig. 4. Lymphocytes and macrophages in *nrf2−/− lpr/lpr* and *nrf2+/+ lpr/lpr* mice lymphnodes. Twenty-week-old *nrf2−/− lpr/lpr* ($N = 4$) and *nrf2+/+ lpr/lpr* ($N = 4$) female mice were used for fluorescence-activated cell sorter (FACS) analysis. Each bar represents the mean ± SEM. $^*P < 0.05$.

lpr/lpr mice. However, there were no difference in apoptotic splenocytes between from *nrf2−/− lpr/lpr* mice and *nrf2+/+ lpr/lpr* mice (data not shown). This result suggested that the immunologic improvements in *nrf2−/− lpr/lpr* mice were not due to an enhancement of Fas-mediated apoptosis. Fas and TNF receptor I (TNF-RI) share homology in their cytoplasmic death domain, a region important for apoptotic signaling [33]. It has been reported that, in *lpr* mice lacking TNF-RI, autoimmunity is greatly accelerated [34]. These facts indicate that TNF-RI might play a compensatory role in Fas-mediated apoptosis in *lpr* mice. Therefore, we examined the effect

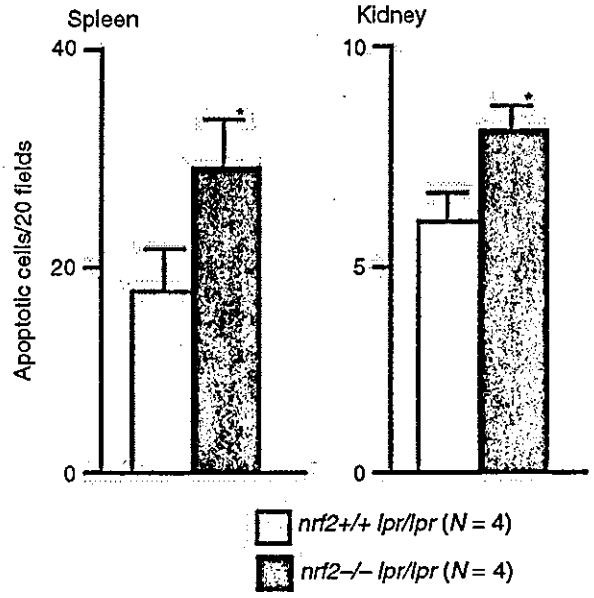

Fig. 5. Detection of apoptotic cells in the spleen of *nrf2−/− lpr/lpr* mice by terminal deoxynucleotidyl transferase (TdT) nick end-labeling (TUNEL) method. Using the TUNEL method, apoptosis was estimated in the spleens and kidneys of 20-week-old *lpr/lpr* female mice. Each bar represents the mean ± SEM. $^*P < 0.05$.

of TNF-α on cultured splenocytes from *nrf2−/− lpr/lpr* mice. We showed that the survival rate of splenocytes from *nrf2−/− lpr/lpr* mice was decreased compared to *nrf2+/+ lpr/lpr* mice ($P < 0.05$) (Fig. 6A). It has been reported that prolonged GSH depletion enhances death receptor (Fas, TNF-RI)–mediated apoptosis [35–37]. We and others reported that intracellular GSH levels were reduced in Nrf2-deficient cells [8, 9]. Moreover, we have reported Nrf2 deficiency increases the sensitivity to Fas and TNF-RI through intracellular glutathione depletion [38]. Therefore, we suspected that the observed sensitivity of TNF-α–mediated apoptosis in *nrf2−/− lpr/lpr* mice could be due to a depletion of cellular GSH levels resulting from a deficiency in Nrf2. GSH-OEt is a compound capable of passing the cell membrane and up-regulating the intracellular levels of GSH [39]. To prove the enhancement of TNF-α–mediated apoptosis in splenocytes from *nrf2 −/− lpr/lpr* mice was due to a decrease in intracellular GSH levels, GSH-OEt was administrated before TNF-α administration. The administration of GSH-OEt increased the survival rate in *nrf2−/− lpr/lpr* mice (Fig. 6B). These results indicate that Nrf2 deficiency can enhance the sensitivity of TNF-α–mediated apoptosis through GSH depletion in vitro.

Hepatocellular apoptosis induction by TNF-α

It is well known that the administration of TNF-α to GalN-sensitized mice can induce fulminant hepatitis as a result of TNF-α–mediated apoptosis [40]. GalN increases the susceptibility of mice to hepatotoxicity and the lethal effects of TNF-α [40]. The effect of hepatocellular apoptosis in vivo triggered by TNF-α in *nrf2−/− lpr/lpr* mice was examined. Serum ALT activity was monitored as indices of hepatotoxicity. We showed that serum ALT activity after TNF-α administration was significantly increased ($P < 0.05$) in *nrf2−/− lpr/lpr* mice compared to *nrf2+/+ lpr/lpr* mice (Table 2).

Histopathologic examination also revealed that apoptotic hepatocytes were increased in *nrf2−/− lpr/lpr* mice (Fig. 6D) compared to *nrf2+/+ lpr/lpr* mice (Fig. 6C). To confirm the enhancement of hepatitis in *nrf2−/− lpr/lpr* mice was due to a decrease in intracellular GSH levels, GSH-OEt was administrated before TNF-α injection. The administration of GSH-OEt decreased the ALT activity in *nrf2−/− lpr/lpr* mice (Table 2). Histopathologic findings also demonstrated GSH-OEt addition rescued *nrf2−/− lpr/lpr* mice from TNF-α–mediated hepatocellular apoptosis (Fig. 6E). Moreover, we performed a quantitative analysis of TUNEL-positive apoptotic cells induced by TNF-α. The number of apoptotic hepatocytes after TNF-α treatment was significantly increased in *nrf2/−/−lpr/lpr* mice ($N = 4$) compared to *nrf2+/+ lpr/lpr* mice ($N = 4$) (Fig. 6F). These results indicate that Nrf2 deficiency can enhance the sensitivity of TNF-α–mediated apoptosis through GSH depletion and that the enhanced sensitivity of TNF-α–mediated apoptosis can improve the immunologic abnormality seen in *lpr* mice.

DISCUSSION

We previously reported that *nrf2* might be one of the candidate genes in determining the susceptibility to autoimmune diseases [12]. MRL/*lpr* mice, having a defect in the Fas molecule, develop spontaneous autoimmune nephritis with generalized peripheral lymphadenopathy [16]. We speculated that *lpr* could stimulate autoimmune disease under conditions where the *nrf2* gene had been deleted. Unexpectedly, this study showed autoimmune nephritis was improved in *nrf2−/− lpr/lpr* mice. Interestingly, we observed that ablation of the *nrf2* gene in *lpr* mice restimulated apoptosis, a response normally blocked as a result of a mutation in *fas*. Fas is expressed at high levels in activated T cells and thought to be critically involved in activation-induced apoptosis in T cells [17, 41–45]. The lymphadenopathy and autoimmune disease seen in MRL/*lpr* mice has been attributed to a defect in Fas-mediated apoptosis in which activated T cells do not undergo activation-induced cell death. In this paper, we clearly demonstrate that apoptotic cells were increased in spleen and kidney in *nrf2−/− lpr/lpr* mice compared with *nrf2+/+ lpr/lpr* mice (Fig. 5). The *lpr* gene consists of a transposon insertion into the *fas* gene resulting in very few Fas molecules being present on the cell surface [16].

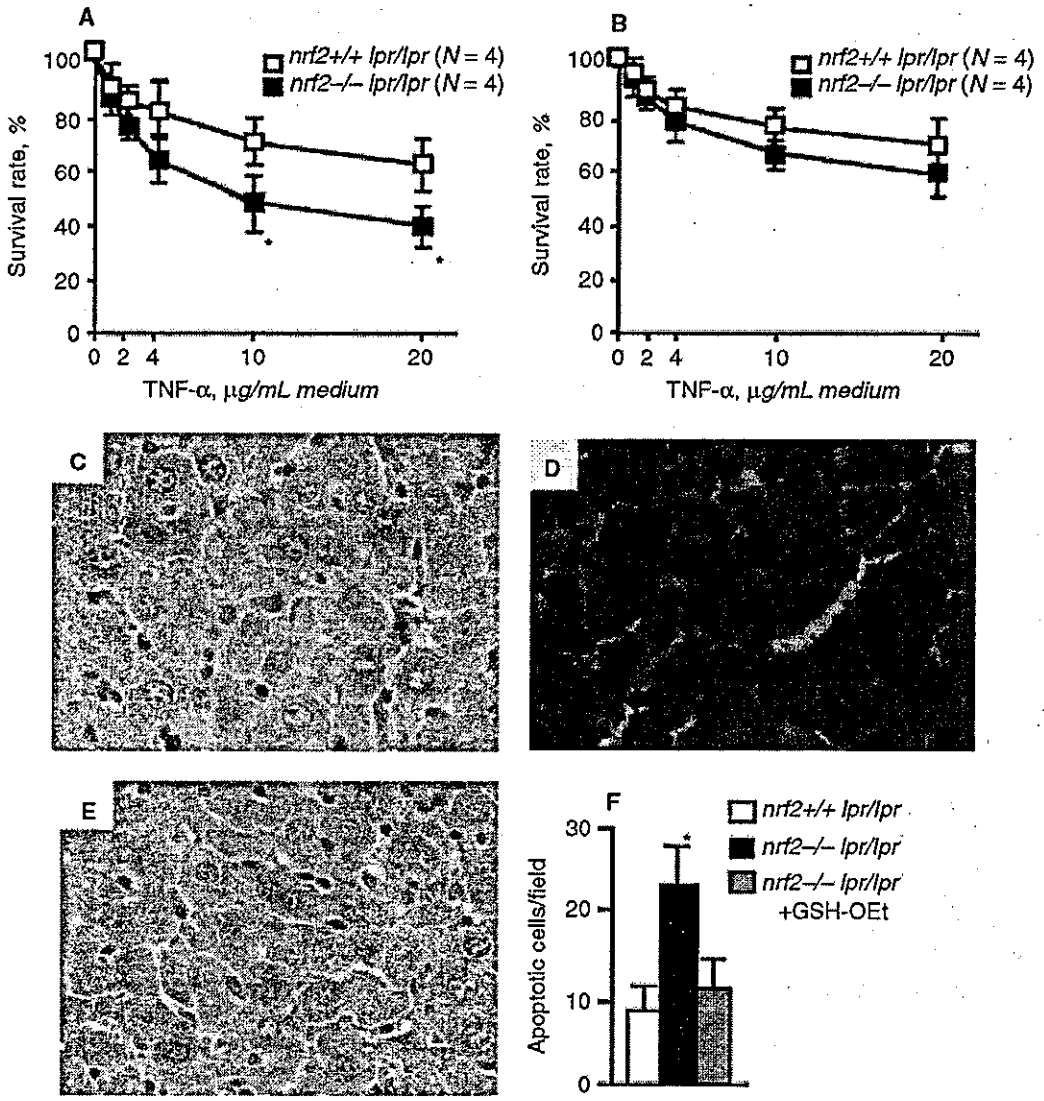

Fig. 6. ***nrf2−/− lpr/lpr*** **mice enhanced tumor necrosis factor-α (TNF-α)–mediated apoptosis whereas administration of glutathione ethyl monoester (GSH-OEt) rescued** ***nrf2−/− lpr/lpr*** **mice from TNF-α–mediated apoptosis.** Effects of Nrf2 deficiency on cultured splenocytes treated with TNF-α. (*A*) Survival rate of *nrf2−/− lpr/lpr* splenocytes after TNF-α stimulation. Each bar represents the mean ± SEM. $^*P < 0.05$. (*B*) GSH-OEt protected *nrf2−/− lpr/lpr* splenocytes against TNF-α–mediated apoptosis. Splenocytes were pre-incubated with 2mM GSH-OEt. (*C*) Liver section from *nrf +/+ lpr/lpr* mouse (×400, hematoxylin and eosin stain). (*D*) *nrf2 −/− lpr/lpr* mouse. Arrows indicate apoptotic nuclei (×400). (*E*) *nrf2−/− lpr/lpr* mouse administered GSH-OEt. The number of apoptotic cells was decreased with GSH-OEt administration (×400). (*F*) Quantitative analysis of terminal deoxynucleotidyl transferase (TdT) nick end-labeling (TUNEL)-positive apoptotic hepatocytes by TNF-α. Each bar represents the mean ± SEM. $^*P < 0.05$.

Therefore, it was possible that the observed improvement of apoptosis in *nrf2−/− lpr/lpr* mice could be due to enhanced sensitivity of Fas-mediated apoptosis. However, the administration of anti-Fas antibody to *nrf2−/− lpr/lpr* splenocytes had no stimulatory effect on apoptosis (data not shown). A further reason for the immunologic improvement seen in the *nrf2−/− lpr/lpr* mice may be a modulation in TNF receptor signaling. Accumulating evidence indicates that TNF signaling is also important for apoptosis. Fas and TNF-RI share a region of homology within their cytoplasmic portions called the death domain, which is responsible for the delivery of intercellular death inducing signals [33]. It has been reported that, in *lpr* mice, substantial numbers of T cells still undergo apoptosis, even though Fas-mediated apoptosis is defective [46]. Further studies have shown that in *lpr* mice lacking TNF-RI, the development of lymphadenopathy and autoantibody production was greatly accelerated compared with TNF-RI wild-type *lpr* mice [34]. These mice also exhibited high mortality and early onset autoimmune disease characterized by massive mononuclear cell infiltration in liver, kidney, lung, and knee joints [34]. These

Table 2. Hepatotoxicity and lethal effect in *nrf2 −/− lpr/lpr* mice induced by tumor necrosis factor-α (TNF-α)[a]

Treatment		Time *hours*	ALT(IU/L)		Survival rate[b]	
			nrf2 −/− lpr/lpr	*nrf2 +/+ lpr/lpr*	*nrf2 −/− lpr/lpr*	*nrf2 +/+ lpr/lpr*
GSH-OEt(−)	TNF-α	0	26.8 ± 3.3	25.2 ± 3.9	5/5	5/5
GSH-OEt(−)	TNF-α	4	761.4 ± 140.0[c]	192.0 ± 45.5	5/5	5/5
GSH-OEt(−)	TNF-α	8	7110.3 ± 882.9[c]	1560.3 ± 145.4	4/5	5/5
GSH-OEt(−)	TNF-α	12	9767.8 ± 867.3[c]	2850.1 ± 348.2	3/5	4/5
GSH-OEt(+)	TNF-α	0	34.2 ± 4.2	28.8 ± 3.7	5/5	5/5
GSH-OEt(+)	TNF-α	4	261.1 ± 55.7	143.8 ± 32.2	5/5	5/5
GSH-OEt(+)	TNF-α	8	1230.3 ± 42.0	925.1 ± 199.6	5/5	5/5
GSH-OEt(+)	TNF-α	12	2565.3 ± 234.8	1235.7 ± 129.8	5/5	5/5

Abbreviations are: ALT, alanine aminotransferase; GSH-OEt, glutathione ethyl monoester; TNF-α, tumor necrosis factor-α.
[a]Results are shown as mean ± SEM for three to five mice; [b]Survival rate indicates the number of survived/all mice; [c]$P < 0.05$.

facts indicate that in *lpr* mice the defects in Fas-mediated apoptosis are exacerbated in the absence of TNF-RI and that normal expression of TNF-RI might partially compensate for the Fas-mediated apoptosis defect of lymphocytes in *lpr* mice. In this study, we demonstrate that Nrf2 deficiency enhanced the sensitivity of TNF-α–mediated apoptosis. Accordingly, an enhanced sensitivity in TNF-α–mediated apoptosis resulting from a deficiency in Nrf2 may have suppressed the accelerating effect of *lpr* in *nrf2−/− lpr/lpr* mice, thereby alleviating the autoimmune disease.

Our study has shown that a deficiency in Nrf2 enhances the sensitivity of TNF-α–mediated apoptosis through a decrease in GSH levels. GSH is an important nonprotein thiol molecule that protects cells against oxidative damage [47, 48]. Nrf2 activates the transcription of the heavy and light chain γ-glutamylcysteine synthetase [GCS (H) and GCS (L)] [8], and cystine membrane transporter (system Xc^-) genes [9] through an ARE/EpRE response element [3, 4]. These molecules are necessary for the synthesis of GSH [8, 9]. An inability to induce the expression of these molecules in Nrf2-deficient mice resulted in increased oxidative stress and the protective response to electrophilic and ROS-producing agents was profoundly impaired [9–11]. Therefore, Nrf2 deficiency resulted in minimum levels of intracellular GSH [9].

Previous reports have shown that a preexisting reduction in GSH levels could significantly increase cell death from TNF-α [49, 50], although the detailed molecular mechanism remains unknown. More recently, we reported that Nrf2 deficiency enhances death-inducing signals through GSH depletion [38]. In our previous study, we found that aged Nrf2-deficient female mice developed autoimmune glomerulonephritis probably due to an increase in oxidative stress [12]. Nephritis in Nrf2-deficient mice develops only in aged females. Therefore, it appears that the *nrf2* gene contributes to the susceptibility to autoimmune disease, rather than acting as an accelerating gene for the disease. In this study, we found that Nrf2 deficiency suppresses the stimulatory effects of the *lpr* gene, which is well known as an accelerating gene for autoimmune diseases. Since this is an unexpected interaction, it is still unclear whether Nrf2 is one of the susceptibility genes for autoimmune diseases. To elucidate the roles of Nrf2 in the development of autoimmune diseases, we will introduce the *nrf2* mutation into BXSB/*Yaa* mice, a disease model not defective for the *fas* gene. This should uncover any synergistic effects that exist between the *Yaa* and *nrf2* mutation.

ACKNOWLEDGMENTS

This work was supported in part by Grants-in-Aid for Scientific Research in Priority Areas and Young Scientists from the Ministry of Education, Culture, Sports, Science and Technology (MEXT), the Japanese Society for Promotion of Sciences (RFTF), Exploratory Research for Advanced Technology (ERATO), and Program for Promotion of Basic Research Activities for Innovative Biosciences (PROBRAIN). We thank Dr. Vincent Kelly for their help and discussion. We also thank N. Kaneko and E. Noguchi (University of Tsukuba) for their excellent assistance.

Reprint requests to Satoru Takahashi, M.D., Ph.D., Institute of Basic Medical Sciences, University of Tsukuba, 1-1-1 Tennodai, Tsukuba City, Ibaraki 305-8575, Japan.
E-mail: satoruta@md.tsukuba.ac.jp

REFERENCES

1. Moi P, Chan K, Asunis I, *et al*: Isolation of NF-E2-related factor 2 (Nrf2), a NF-E2-like basic leucine zipper transcriptional activator that binds to the tandem NF-E2/AP1 repeat of the β-globin locus control region. *Proc Natl Acad Sci USA* 91:9926–9930, 1994
2. Itoh K, Igarashi K, Hayashi N, *et al*: Cloning and characterization of a novel erythroid cell-derived CNC family transcription factor heterodimerizing with the small Maf family proteins. *Mol Cell Biol* 15:4184–4193, 1995
3. Itoh K, Ishii T, Wakabayashi N, Yamamoto M: Regulatory mechanisms of cellular response to oxidative stress. *Free Radic Res* 31:319–324, 1999
4. Itoh K, Chiba T, Takahashi S, *et al*: An Nrf2/small Maf heterodimer mediates the induction of phase II detoxifying enzyme genes through antioxidant response elements. *Biochem Biophys Res Commun* 236:313–322, 1997
5. Rushmore TH, King RG, Paulson KE, Pickett CB: Regulation of glutathione S-transferase Ya subunit gene expression: Identification of a unique xenobiotic-responsive element controlling inducible expression by planar aromatic compounds. *Proc Nat Acad Sci USA* 87:3826–3830, 1990
6. Favreau LV, Pickett CB: Transcriptional regulation of the rat NAD(P)H: Quinone reductase gene. *J Biol Chem* 266:4556–4561, 1991

7. Prestera T, Talalay P, Alam J, *et al*: Parallel induction of heme oxygenase-1 and chemoprotective phase 2 enzymes by electrophiles and antioxidants: Regulation by upstream antioxidant-responsive elements (ARE). *Mol Med* 1:827–837, 1995
8. Mulcahy RT, Wartman MA, Bailey HH, Gipp JJ: Constitutive and naphthoflavone-induced expression of the human γ-glutamylcysteine synthetase heavy subunit gene is regulated by a distal antioxidant response element/TRE sequence. *J Biol Chem* 272:7445–7454, 1997
9. Ishii T, Itoh K, Takahashi S, *et al*: Transcription factor Nrf2 coordinately regulates a group of oxidative stress-inducible genes in macrophages. *J Biol Chem* 275:16023–16029, 2000
10. Cho HY, Jedlicka AE, Reddy SP, *et al*: Role of NRF2 in protection against hyperoxic lung injury in mice. *Am J Respir Cell Mol Biol* 26:175–182, 2002
11. Enomoto A, Itoh K, Nagayoshi E, *et al*: High sensitivity of Nrf2 knockout mice to acetaminophen hepatotoxicity associated with decreased expression of ARE-regulated drug metabolizing enzymes and antioxidant genes. *Toxicol Sci* 59:169–177, 2001
12. Yoh K, Itoh K, Enomoto A, *et al*: Nrf2-deficient female mice develop lupus-like autoimmune nephritis. *Kidney Int* 60:1343–1353, 2001
13. Murphy ED, Roths JB: Autoimmunity and lymphoproliferation: Induction by mutant gene *lpr*, and acceleration by a male-associated factor in strain BXSB mice, in *Genetic Control of Autoimmune Disease*, edited by Rose NR, Bigazzi PE, Warner NL, New York, Elsevier, 1978, pp 207–221
14. Helyer BJ, Howie JB: Renal disease associated with positive lupus erythematosus tests in a crossbred strain of mice. *Nature* 197:197, 1963
15. Andrews BS, Eisenberg RA, Theofilopoulos AN, *et al*: Spontaneous murine lupus-like syndromes: Clinical and immunopathological manifestations in several strains. *J Exp Med* 148:1198–1215, 1978
16. Watanabe-Fukunaga R, Brannan CI, Copeland NG, *et al*: Lymphoproliferation disorder in mice explained by defects in Fas antigen that mediates apoptosis. *Nature* 356:314–317, 1992
17. Russell JH, Rush B, Weaver C, *et al*: Mature T cells of autoimmune *lpr/lpr* mice have a defect in antigen-stimulated suicide. *Proc Natl Acad Sci USA* 90:4409–4413, 1993
18. Cohen PL, Eisenberg RA: *lpr* and *gld*: Single gene models of systemic autoimmunity and lymphoproliferative disease. *Annu Rev Immunol* 9:243–269, 1991
19. Takahashi S, Nose M, Sasaki J, *et al*: IgG3 production in MRL/*lpr* mice is responsible for development of lupus nephritis. *J Immunol* 147:515–519, 1991
20. Izui S, Kelley VE, Masuda K, *et al*: Induction of various autoantibodies by mutant gene *lpr* in several strains of mice. *J Immunol* 133:227–233, 1984
21. Nose M, Nishimura M, Ito MR, *et al*: Arteritis in a novel congenic strain of mice derived from MRL/*lpr* lupus mice: genetic dissociation from glomerulonephritis and limited autoantibody production. *Am J Pathol* 149:1763–1769, 1996
22. Iwata Y, Wada T, Furuichi K, *et al*: p38 Mitogen-activated protein kinase contributes to autoimmune renal injury in MRL-Fas *lpr* mice. *J Am Soc Nephrol* 14:57–67, 2003
23. Sasaki T, Muryoi T, Sekiguchi Y, *et al*: Monoclonal human anti-DNA antibodies from EB virus-transformed lymphocytes of systemic lupus erythematosus (SLE) patients. *J Clin Immunol* 5:246–253, 1985
24. Jevnikar AM, Grusby MJ, Glimcher LH: Prevention of nephritis in major histocompatibility complex class II-deficient MRL-*lpr* mice. *J Exp Med* 179:1137–1143, 1994
25. Kikawada E, Lenda DM, Kelley VR: IL-12 deficiency in MRL-Fas (*lpr*) mice delays nephritis and intrarenal IFN-gamma expression, and diminishes systemic pathology. *J Immunol* 170:3915–3925, 2003
26. Schwarting A, Wada T, Kinoshita K, *et al*: IFN-gamma receptor signaling is essential for the initiation, acceleration, and destruction of autoimmune kidney disease in MRL-Fas (*lpr*) mice. *J Immunol* 161:494–503, 1998
27. Yokoyama H, Kreft B, Kelley VR: Biphasic increase in circulating and renal TNF-alpha in MRL-*lpr* mice with differing regulatory mechanisms. *Kidney Int* 47:122–130, 1995
28. Wada T, Naito T, Griffiths RC, *et al*: Systemic autoimmune nephritogenic components induce CSF-1 and TNF-alpha in MRL kidneys. *Kidney Int* 52:934–941, 1997
29. Yamamoto K, Loskutoff DJ: Expression of transforming growth factor-beta and tumor necrosis factor-alpha in the plasma and tissues of mice with lupus nephritis. *Lab Invest* 80:1561–1570, 2000
30. Balomenos D, Rumold R, Theofilopoulos AN: Interferon-gamma is required for lupus-like disease and lymphoaccumulation in MRL-*lpr* mice. *J Clin Invest* 101:364–371, 1998
31. Carvalho-Pinto CE, Garcia MI, *et al*: Autocrine production of IFN-gamma by macrophages controls their recruitment to kidney and the development of glomerulonephritis in MRL/*lpr* mice. *J Immunol* 169:1058–1067, 2000
32. Fossati L, Takahashi S, Merino R, *et al*: An MRL/MpJ-*lpr/lpr* substrain with a limited expansion of *lpr* double-negative T cells and a reduced autoimmune syndrome. *Int Immunol* 5:525–532, 1993
33. Tartaglia LA, Ayres TM, Wong GH, *et al*: A novel domain within the 55 kd TNF receptor signals cell death. *Cell* 74:845–853, 1993
34. Zhou T, Edwards CK, Yang P, *et al*: Greatly accelerated lymphadenopathy and autoimmune disease in *lpr* mice lacking tumor necrosis factor receptor I. *J Immunol* 156:2661–2665, 1996
35. Chiba T, Takahashi S, Sato N, *et al*: Fas-mediated apoptosis is modulated by intracellular glutathione in human T cells. *Eur J Immunol* 26:1164–1169, 1996
36. Xu Y, Jones BE, Neufeld DS, Czaja MJ: Glutathione modulates rat and mouse hepatocyte sensitivity to tumor necrosis factor toxicity. *Gastroenterology* 115:1229–1237, 1998
37. Colell A, Garcia-Ruiz C, Miranda M, *et al*: Selective glutathione depletion of mitochondria by ethanol sensitizes hepatocytes to tumor necrosis factor. *Gastroenterology* 115:1541–1551, 1998
38. Morito N, Yoh K, Itoh K, *et al*: Nrf2 regulates the sensitivity of death receptor signals through intra-cellular glutathione levels. *Oncogene* 22:9275–9281, 2003
39. Chen TS, Richie JP, Nagasawa HT, Lang CA: Glutathione monoethyl ester protects against glutathione deficiencies due to aging and acetaminophen in mice. *Mech Ageing Dev* 120:127–139, 2000
40. Tiegs G, Wolter M, Wendel A: Tumor necrosis factor is a terminal mediator in galactosamine/endotoxin-induced hepatitis in mice. *Biochem Pharmacol* 38:627–631, 1989
41. Green DR, Scott DW: Activation-induced apoptosis in lymphocytes. *Curr Opin Immunol* 6:476–487, 1994
42. Westendorp MO, Frank R, Ochsenbauer C, *et al*: Sensitization of T cells to CD95-mediated apoptosis by HIV-1 Tat and gp120. *Nature* 375:497–500, 1995
43. Brunner T, Mogil RJ, LaFace D, *et al*: Cell-autonomous Fas (CD95)/Fas ligand interaction mediates activation-induced apoptosis in T-cell hybridomas. *Nature* 373:441–444, 1995
44. Rothstein TL, Wang JK, Panka DJ, *et al*: Protection against Fas-dependent Th1-mediated apoptosis by antigen receptor engagement in B cells. *Nature* 374:163–165, 1995
45. Vignaux F, Vivier E, Malissen B, *et al*: TCR/CD3 coupling to Fas-based cytotoxicity. *J Exp Med* 181:781–786, 1995
46. Adachi M, Suematsu S, Suda T, *et al*: Enhanced and accelerated lymphoproliferation in Fas-null mice. *Proc Natl Acad Sci USA* 93:2131–2136, 1996
47. Meister A: On the antioxidant effects of ascorbic acid and glutathione. *Biochem Pharmacol* 44:1905–1915, 1992
48. Meister A, Larsson CR, Scriver AL, *et al*: *The Metabolic and Molecular Basis of Inherited Disease*, New York, McGraw-Hill, 1995, pp1461–1477
49. Colell A, Garcia-Ruiz C, Miranda M, *et al*: Selective glutathione depletion of mitochondria by ethanol sensitizes hepatocytes to tumor necrosis factor. *Gastroenterology* 115:1541–1551, 1998
50. Yang XU, Jones BE, Neufeld DS, Czaja MJ: Glutathione modulates rat and mouse hepatocyte sensitivity to tumor necrosis factor toxicity. *Gastroenterology* 115:1229–1237, 1998

THE JOURNAL OF BIOLOGICAL CHEMISTRY
Vol. 279, No. 24, Issue of June 11, pp. 25204–25210, 2004
Printed in U.S.A.

A Constitutively Active Arylhydrocarbon Receptor Induces Growth Inhibition of Jurkat T Cells through Changes in the Expression of Genes Related to Apoptosis and Cell Cycle Arrest*

Received for publication, February 26, 2004, and in revised form, March 23, 2004
Published, JBC Papers in Press, April 6, 2004, DOI 10.1074/jbc.M402143200

Tomohiro Ito‡, Shin-ichi Tsukumo‡, Norio Suzuki§, Hozumi Motohashi§, Masayuki Yamamoto§, Yoshiaki Fujii-Kuriyama§, Junsei Mimura§, Tien-Min Lin¶, Richard E. Peterson¶, Chiharu Tohyama‡, and Keiko Nohara‡‖

From the ‡Environmental Health Sciences Division, National Institute for Environmental Studies, Tsukuba 305-8506, Japan, the §Center for Tsukuba Advanced Research Alliance, University of Tsukuba, Tsukuba 305-8575, Japan, and the ¶School of Pharmacy, University of Wisconsin, Madison, Wisconsin 53705

2,3,7,8-Tetrachlorodibenzo-*p*-dioxin (TCDD) is known to suppress T cell-dependent immune reactions through the activation of the arylhydrocarbon receptor (AhR). Our previous findings suggest that TCDD inhibits the activation and subsequent expansion of T cells following antigen stimulation in mice, leading to a decreased level of T cell-derived cytokines involved in antibody production. In the present study, we investigated the effects of activated AhR on T cells by transiently expressing a constitutively active AhR (CA-AhR) mutant in AhR-null Jurkat T cells. In agreement with our previous findings, CA-AhR markedly inhibited the growth of Jurkat T cells. The inhibited cell growth was found to be concomitant with both an increase in the annexin V-positive apoptotic cells and the accumulation of cells in the G_1 phase. The growth inhibition was also shown to be mediated by both xenobiotic response element (XRE)-dependent and -independent mechanisms, because an A78D mutant of the CA-AhR, which lacks the ability of XRE-dependent transcription, partially inhibited the growth of Jurkat T cells. Furthermore, we demonstrated that CA-AhR induces expression changes in genes related to apoptosis and cell cycle arrest. These expression changes were shown to be solely mediated in an XRE-dependent manner, because the A78D mutant of the CA-AhR did not induce them. To summarize, these results suggest that AhR activation causes apoptosis and cell cycle arrest, especially through expression changes in genes related to apoptosis and cell cycle arrest by the XRE-dependent mechanism, leading to the inhibition of T cell growth.

2,3,7,8-Tetrachlorodibenzo-*p*-dioxin (TCDD)[1] is known to exert a variety of toxicities such as reproductive toxicity, immunotoxicity, teratogenicity, and neurotoxicity (1, 2). Previous studies using arylhydrocarbon receptor (AhR) knock-out mice indicate that most, if not all, of the TCDD-induced toxicity is mediated by the AhR, a basic helix-loop-helix periodicity/ARNT/single-minded (PAS) transcription factor (3, 4). In the absence of a ligand, the AhR is located in the cytoplasm in association with heat shock protein 90, X-associated protein 2, and heat shock protein 90 co-chaperone p23 (5). Once a ligand, such as TCDD, binds to the AhR, the complex is translocated into the nucleus where it forms a heterodimer with an AhR nuclear translocator (ARNT). The AhR/ARNT heterodimer binds to specific DNA sequences termed xenobiotic response elements (XREs), and it enhances the expression of genes such as cytochrome P-450 1A1 (*CYP1A1*) (4, 6). On the other hand, it has also been shown that the ligand-activated AhR directly interacts with retinoblastoma protein (RB) (7, 8) and NF-κB (RelA) (9), and their direct interactions modulate the signaling pathways involved in many physiological functions. Although many studies have been conducted, the precise mechanism for individual toxicities of TCDD remains to be clarified.

As regards immunotoxicity, TCDD induces thymus atrophy and suppresses both humoral and cellular immunity in an AhR-dependent manner (10, 11). Recent studies using chimeric mice with the AhR in either hemopoietic or stromal tissues showed that TCDD induces thymus atrophy by directly affecting thymocytes (immature T cells) and not dendritic or stromal cells (12, 13). Additionally, it has been suggested that TCDD-induced thymus atrophy can be attributed to the inhibition of G_1/S cell cycle progression in thymocytes at the double negative stages of T cell development (12). In terms of cellular immunity, it has been reported that full suppression of the cytotoxic T lymphocyte response by TCDD required AhR expression in both $CD4^+$ and $CD8^+$ T cells; this indicates that T cells are direct targets of TCDD (14). With regard to the suppressive effect of TCDD on humoral immunity, primary effects on both B cells and T cells have been reported by several groups (11, 15). Recently, we showed that TCDD considerably reduces the production of the T cell growth factor IL-2 and $CD4^+$ type 2 helper T cell-derived cytokines prior to the inhibition of antibody suppression in mice immunized with ovalbumin (16–18). Furthermore, TCDD suppressed the increase in the number of T cells in the spleen, following immunization. This suggests

* This work was supported by grants from the Core Research for Evolutional Science and Technology, Japan Science and Technology Agency (to C. T., K. N., T. I., and S. T.) and the Ministry of the Environment. The costs of publication of this article were defrayed in part by the payment of page charges. This article must therefore be hereby marked "*advertisement*" in accordance with 18 U.S.C. Section 1734 solely to indicate this fact.

‖ To whom correspondence should be addressed: National Institute for Environmental Studies, Tsukuba 305-8506, Japan. Tel.: 81-29-850-2500; Fax: 81-29-850-2574; E-mail: keikon@nies.go.jp.

[1] The abbreviations used are: TCDD, 2,3,7,8-tetrachlorodibenzo-*p*-dioxin; AhR, arylhydrocarbon receptor; ARNT, arylhydrocarbon receptor nuclear translocator; XRE, xenobiotic response element; CA-AhR, constitutively active arylhydrocarbon receptor; PAS, periodicity/ARNT/single-minded; RB, retinoblastoma protein; IL-2, interleukin-2; GFP, green fluorescent protein; PI, propidium iodide; RT, reverse transcriptase; CYP1A1, cytochrome P-450 1A1; FACS, fluorescence-activate cell sorting; TGF, transforming growth factor; CDA1, cell division autoantigen-1; GADD45A, growth arrest and DNA-damage-inducible, alpha.

that TCDD inhibits the activation of antigen-specific T cells and their subsequent expansion, which probably leads to deteriorated antibody production (16). All these findings strongly suggest that T cells are a vulnerable target of TCDD toxicity, with regard to not only thymus atrophy and inhibition of cellular immunity but also the suppression of humoral immunity. Our recent finding that primary T cells have functional AhR also supports this mechanism (19).

In the present study, to investigate the effects of activated AhR on T cells and their underlying mechanism, we transiently expressed a constitutively active AhR (CA-AhR) mutant in human leukemic Jurkat T cells, because all the T cell lines examined thus far, including Jurkat T cells, do not have functional AhR (20, 21). We used a CA-AhR mutant lacking the minimal PAS B motif, which is constitutively localized in the nucleus and activates AhR-dependent transcription independent of the ligand (22, 23). We also generated an A78D mutant of the CA-AhR, which lacks the ability of XRE-dependent transcription (24), and examined the involvement of XRE-dependent transcription in the effects of CA-AhR on Jurkat T cells.

EXPERIMENTAL PROCEDURES

Plasmid Construction—pEB6CAGFP (an Epstein-Barr virus-based expression vector for green fluorescent protein (GFP) driven by a CAG promoter) (25) and pEB6CAGMCS (containing multicloning sites) were kindly provided by Dr. Yoshihiro Miwa (University of Tsukuba, Tsukuba, Japan). A CA-AhR cDNA[2] was subcloned into a KpnI-HindIII site of pEB6CAGMCS, and pEB6CAG-CA-AhR-GFP, encoding a CA-AhR fused to GFP, was generated by inserting the SalI-AflII fragment of pEGFP-N3 (Clontech Laboratories, Inc., Palo Alto, CA). To examine whether the effects of CA-AhR on Jurkat T cells are mediated by XRE-dependent transcription, the mutation changing the alanine at position 78 to aspartic acid (A78D) (24) in the CA-AhR was introduced by the use of a QuikChange XL site-directed mutagenesis kit (Stratagene, La Jolla, CA) according to the manufacturer's instructions. A primer with the sequence 5′-GTCAGCTACCTGAGGGACAAGAGCTTCTTTGATG-3′ and its complementary equivalent were employed.

Cell Line, Transient Transfection, and Sorting—Jurkat T cells were obtained from the Cell Resource Center for Biomedical Research (Tohoku University, Sendai, Japan) and maintained in RPMI 1640 (Sigma) supplemented with 10% heat-inactivated fetal bovine serum (Invitrogen), 10 mM HEPES (pH 7.1), 1 mM pyruvate, and 50 μM 2-mercaptoethanol at 37 °C in 5% CO_2. Jurkat T cells (2×10^6 cells) were transiently transfected with 6 μg of pEB6CAGFP, pEB6CAG-CA-AhR-GFP, or pEB6CAG-A78D-GFP using DMRIE-C reagent (Invitrogen) according to the manufacturer's instructions. After 2 days, GFP-positive cells from each transfectant were sorted using a FACSVantage SE (BD Biosciences). The efficiency of the sorting was confirmed using a FACSCalibur (BD Biosciences), and 98–99% of the sorted cells were GFP-positive. The sorted cells were cultured at 1×10^5 cells/ml, and then growth rate, apoptosis, and cell cycle distribution were examined as described below. The results obtained in each experiment were confirmed in another independent experiment, and a set of representative results has been shown under "Results."

Detection of Apoptosis—For the detection of apoptotic cells by annexin V binding and propidium iodide (PI) staining, we used an Annexin V-biotin apoptosis detection kit (BioVision, Palo Alto, CA) according to the manufacturer's instructions, with minor modifications. At 0, 2, and 4 days after sorting, the cells were incubated with biotin-labeled annexin V for 5 min at room temperature. After washing, the cells were incubated with streptavidin-labeled allophycocyanin (SA-APC, BD Biosciences) for 15 min at room temperature. After washing, PI was added, and the cells were analyzed using a FACSCalibur.

Furthermore, the induction of apoptosis was confirmed by apoptotic morphological changes. The sorted cells were cultured for 2 days and then stained with 4 μM bisbenzimide (Hoechst 33342, ICN Biomedicals Inc., Aurora, OH) for 15 min. The apoptotic cells were examined by the changes in their nuclear morphology, *i.e.* nuclear fragmentation, under a UV-visible fluorescence microscope. Approximately over 100 cells were counted in four microscopic fields, and the percentage of apoptotic cells was estimated.

Cell Cycle Analysis—At 0, 2, and 4 days after sorting, the cells were stained with PI using a CycleTEST Plus DNA reagent kit (BD Biosciences) according to the manufacturer's instructions, and their DNA content was measured using a FACSCalibur. The percentages of cells in the G_1, S, and G_2/M phases were analyzed using ModFit software (BD Biosciences).

Affymetrix GeneChip Analysis—Affymetrix GeneChip analysis was performed according to the Affymetrix expression analysis technical manual (Affymetrix, Santa Clara, CA), with some modifications. After sorting, total RNA was isolated using an RNeasy Mini Kit (Qiagen, Chatsworth, CA). Double-stranded cDNA was synthesized from 1 μg of total RNA using SuperScript II reverse transcriptase (Invitrogen) and T7 oligo$(dT)_{24}$ primer (Affymetrix). The double-stranded cDNA was purified by the phenol/chloroform extraction method, followed by ethanol precipitation. The *in vitro* transcription reaction was performed using a BioArray high yield RNA transcript-labeling kit (Enzo Diagnostics, Farmingdale, NY). 15 μg of the biotin-labeled cRNA was fragmented and hybridized to a Human Genome U133A array (Affymetrix). The hybridized probe array was washed, stained, and scanned. The data were analyzed using Affymetrix Microarray Suite 5.0 software. A comparison analysis was performed to obtain genes with at least 2-fold changes in Jurkat T cells expressing CA-AhR-GFP as compared with cells expressing GFP alone.

Semiquantitative RT-PCR—To confirm the gene expression changes observed by the Affymetrix GeneChip analysis, semiquantitative RT-PCR was performed on the double strand cDNA prepared for Affymetrix GeneChip analysis. Primers used in the present study were designed using PRIMER3 (frodo.wi.mit.edu/cgi-bin/primer3/primer3_www.cgi) and NCBI UniSTS (www.ncbi.nlm.nih.gov/entrez/query.fcgi?db=unists), based on human sequences published in the NCBI data base. Primer sequences, PCR cycle numbers, and the annealing temperatures of each gene are shown in Table I. Each double-stranded cDNA was amplified in the exponential phase of PCR using TaKaRa *Taq* (TaKaRa Shuzo Co., Ltd., Tokyo, Japan). The amplification was carried out by an initial incubation at 94 °C for 2 min, followed by 19–30 cycles of 94 °C for 30 s, 55 or 60 °C for 30 s, and 72 °C for 30 s, and a final extension at 72 °C for 7 min. The PCR products were separated in a 1.2% Synergel (Diversified Biotech, Boston, MA) containing 0.5 μg/ml ethidium bromide. The net intensity of the bands was quantified using Kodak EDAS 290. The expression level of each gene was normalized to that of glyceraldehyde-3-phosphate dehydrogenase or β-actin.

RESULTS

CA-AhR Inhibits Growth of Jurkat T Cells—To examine the effect of AhR activation on T cells, we used a CA-AhR mutant lacking the minimal PAS B motif (Fig. 1*A*). The CA-AhR mutant has been reported to form a heterodimer with ARNT and induce XRE-dependent gene expression in Chinese hamster ovary cells and MCF-7 cells in the absence of a ligand (22, 23). First, we examined CYP1A1 expression to confirm that CA-AhR induces XRE-dependent gene expression in Jurkat T cells. Jurkat T cells, which expressed ARNT but not AhR (data not shown), were transiently transfected with an expression vector for either CA-AhR-GFP or GFP alone. Two days after the transfection, GFP-positive cells were sorted and RT-PCR for CYP1A1 mRNA was performed. As shown in Fig. 1*B*, CA-AhR-GFP, but not GFP alone, markedly induced CYP1A1 mRNA expression, indicating that the CA-AhR is functional in Jurkat T cells. In addition, the green fluorescence emitted from CA-AhR-GFP was mainly found in the nuclear compartment (data not shown).

To examine the effect of CA-AhR on the growth rate of Jurkat T cells, the sorted cells were cultured for up to 4 days, and the cell numbers were counted at the indicated times. As shown in Fig. 2, the cells expressing GFP alone increased 10-fold, 4 days after sorting. In contrast, the expression of CA-AhR-GFP completely inhibited the increase in cell numbers up to 4 days after sorting, indicating that the activation of AhR greatly inhibits the growth of Jurkat T cells.

CA-AhR Induces Apoptosis in Jurkat T Cells—Because CA-AhR was shown to induce growth inhibition, we examined whether the expression of CA-AhR induces apoptosis in Jurkat T cells. Apoptotic cells were detected with annexin V, which monitors the appearance of phosphatidylserine on the cell sur-

[2] Y. Fujii-Kuriyama and J. Mimura, unpublished data.

TABLE I
List of primers used for semiquantitative RT-PCR

Description	GenBank™ accession number	Primer sequence (5′–3′)	PCR cycle number	Annealing temperature	Product size
				°C	*bp*
AhR	L19872	TTACCTGGGCTTTCAGCAGT AACTGGGGTGGAAAGAATCC	19	60	506 (CA-AhR)
β-Actin	X00351	GAGGCCCAGAGCAAGAGAG GGCTGGGGTGTTGAAGGT	19	60	225
Caspase 8	U58143	CTTGGATGCAGGGGCTTTGACC GTTCACTTCAGTCAGGATGG	23	55	550
CDA1	AF254794	TGAGGAGGAAGGAAGTGAAGA TAGTGGGTGGGGGATACAGA	26	60	171
c-Jun	BC002646	GGTATCCTGCCCAGTGTTGT CGCACTAGCCTTTGGTAAGC	25	60	382
c-Myc	V00568	TCGGATTCTCTGCTCTCCTC CGCCTCTTGACATTCTCCTC	24	60	413
Cyclin G2	U47414	TGGACAGGTTCTTGGCTCTT AATACAGATGGTTTTGCTTTTGA	28	55	367
CYP1A1	X02612	CTTGGACCTCTTTGGAGCTG CGAAGGAAGAGTGTCGGAAG	30	60	212
DUSP6	AB013382	CGATGAACGATGCCTATGAC TGCCAAGAGAAACTGCTGAA	29	60	262
Fas	M67454	CTGCCATAAGCCCTGTCCT CAAAGCCACCCCAAGTTAGA	27	60	360
GADD34	U83981	CCTCCTCTGTCCCTTCGTC AGTTGGTCTCAGCCACGC	26	60	127
GADD45A	M60974	CTGGAGGAAGTGCTCAGCAAAG TTGATCCATGTAGCGACTTTCC	27	60	399
GAPDH	M33197	ACCACAGTCCATGCCATCAC TCCACCACCCTGTTGCTGTA	19	60	452
IL-9 receptor	M84747	TTCACCATCACTTTCCACCA AACGCTCCTCCTCTACCACA	26	60	370
$p21^{waf1}$	U03106	GGGAAGGGACACACAAGAAG GGGAGCCGAGAGAAAACAG	25	60	478
TGF-β receptor II	D50683	CGGCTCCCTAAACACTACCA GGTCCCTTCCTTCTCTGCTT	27	60	478

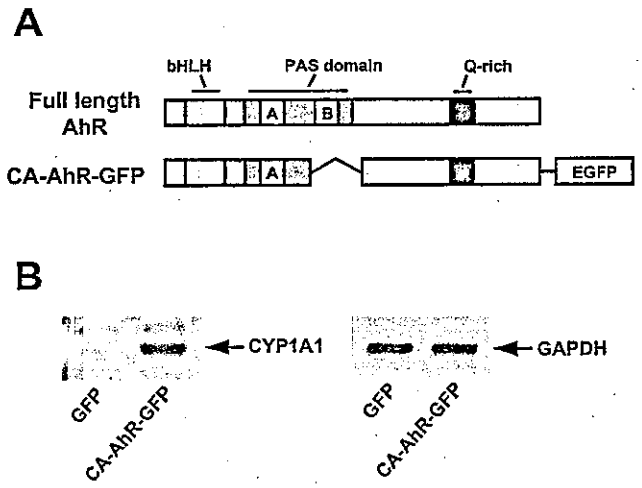

FIG. 1. **Structure of a constitutively active mutant of an aryl-hydrocarbon receptor (CA-AhR) and CYP1A1 induction in Jurkat T cells expressing CA-AhR.** *A*, the structures of wild-type AhR and a CA-AhR fused to GFP (CA-AhR-GFP) are shown. The CA-AhR lacks the minimal PAS B motif. *B*, the expression vector for either CA-AhR-GFP or GFP alone was transiently transfected into Jurkat T cells using DMRIE-C reagent. Two days after transfection, GFP-positive cells were sorted using a FACSVantage SE. Total RNA was isolated from the cells, and mRNA expression levels of CYP1A1 and glyceraldehyde-3-phosphate dehydrogenase were examined by semiquantitative RT-PCR.

face during apoptosis. In addition, PI was used to distinguish between early and late apoptosis, because PI is excluded only by live and early apoptotic cells. As shown in Fig. 3, where annexin V-positive, PI-negative cells (*upper left quadrant*) represent early apoptotic cells and annexin V, PI-double positive

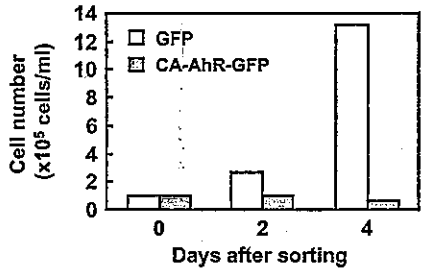

FIG. 2. **CA-AhR inhibits growth of Jurkat T cells.** The expression vector for either CA-AhR-GFP or GFP alone was transiently transfected into Jurkat T cells using DMRIE-C reagent. After 2 days, GFP-positive cells from each transfected cells were sorted using a FACSVantage SE and then cultured at 1×10^5 cells/ml. The cell numbers at the indicated times were determined by trypan blue exclusion.

cells (*upper right quadrant*) represent late apoptotic/necrotic cells, GFP-alone-transfected cells did not show remarkable changes in the ratio of dead cells. On the other hand, CA-AhR-GFP increased the percentage of apoptotic cells, especially 2 and 4 days after sorting. Two days after sorting, the percentage of early apoptotic cells was 3-fold higher in cells expressing CA-AhR-GFP than in those expressing GFP alone. Moreover, 4 days after sorting, CA-AhR-GFP augmented the percentages of early apoptotic cells and late apoptotic/necrotic cells by approximately 8- and 6-fold, respectively, as compared with GFP alone.

Furthermore, the induction of apoptosis was confirmed by nuclear morphological changes. Each group of sorted cells was cultured for 2 days and stained with Hoechst 33342 dye. Fragmented nuclei were observed in a number of cells expressing CA-AhR-GFP (Fig. 4*A*, *arrowheads*), and apoptotic cells reached about 30%; however, the apoptotic cells only reached 10% in cells expressing GFP alone (Fig. 4*B*).

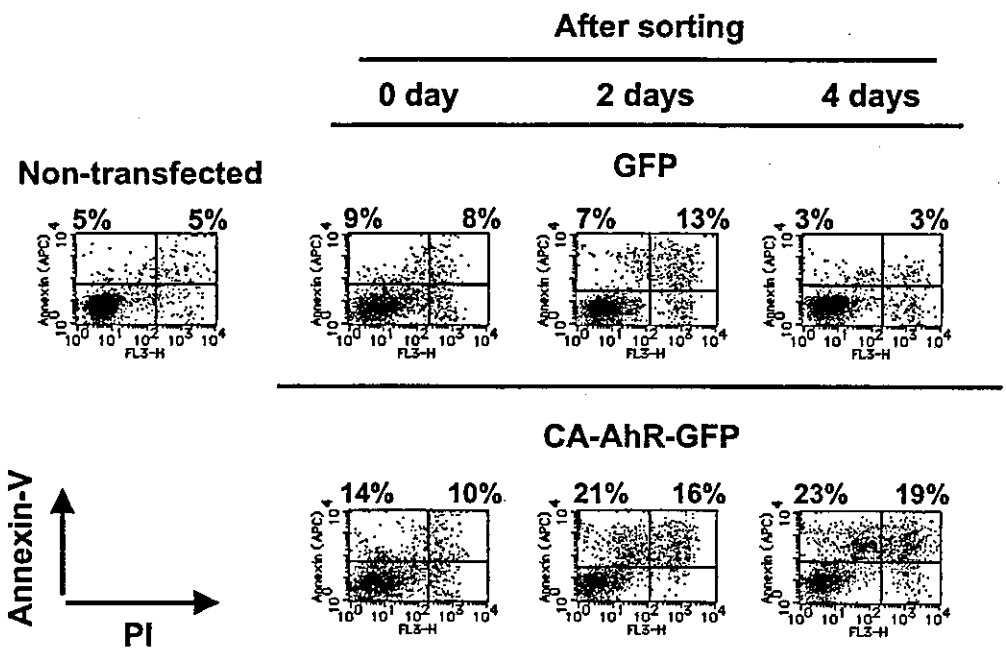

FIG. 3. **CA-AhR induces apoptosis in Jurkat T cells.** The expression vector for either CA-AhR-GFP or GFP alone was transiently transfected into Jurkat T cells using DMRIE-C reagent. After 2 days, GFP-positive cells were sorted from the transfected cells using a FACSVantage SE and then cultured for the indicated time periods. The cells were incubated with biotin-labeled annexin V, followed by staining with SA-APC and PI, and analyzed using a FACSCalibur. The *upper left quadrant* (annexin V-positive, PI-negative) represents early apoptotic cells, whereas the *upper right quadrant* (annexin V, PI-double positive) represents late apoptotic/necrotic cells.

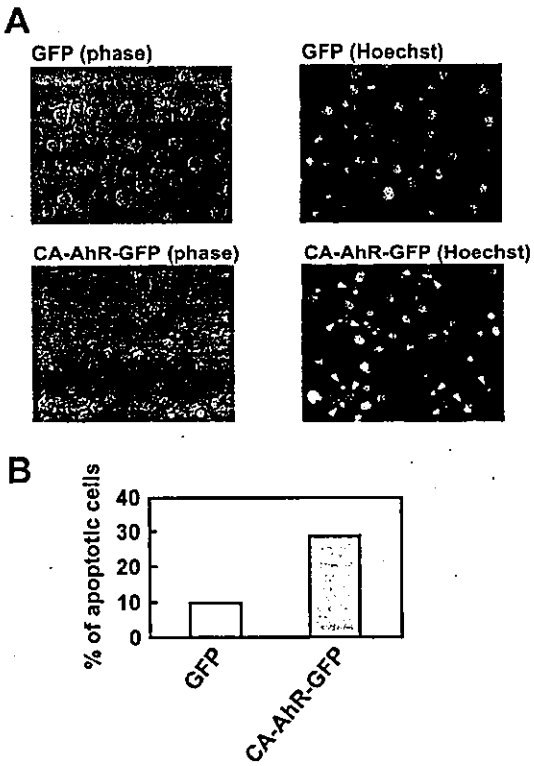

FIG. 4. **CA-AhR induces apoptotic morphological changes in Jurkat T cells.** *A*, the expression vector for either CA-AhR-GFP or GFP alone was transiently transfected into Jurkat T cells using DMRIE-C reagent. After 2 days, GFP-positive cells were sorted from the transfected cells using a FACSVantage SE. The sorted cells were cultured for 2 days and then stained with 4 μM Hoechst 33342 for 15 min. The apoptotic cells were examined by the changes in their nuclear morphology, *i.e.* with fragmentation under a phase-contrast and a UV-visible fluorescence microscope. The *arrowheads* indicate the fragmented nuclei of the apoptotic cells. *B*, approximately over 100 cells were counted in four microscopic fields under a UV-visible fluorescence microscope, and the percentage of the apoptotic cells was estimated.

CA-AhR Induces the Accumulation of Cells in the G_1 Phase—We also investigated the possibility that CA-AhR induces cell cycle arrest. As shown in Fig. 5, in non-transfected Jurkat T cells, 48% of the cells were in the G_1 phase, 37% were in the S phase, and 15% were in the G_2/M phase. Immediately after sorting (0 day), no difference was observed in the DNA profile among non-transfected cells, cells expressing GFP alone, and those expressing CA-AhR-GFP. Two days after sorting, the percentage of cells expressing CA-AhR-GFP rose to 61% in the G_1 phase and correspondingly decreased to 24% in the S phase, whereas no change in cell cycle distribution was observed in cells expressing GFP alone. Four days after sorting, the percentages in the individual phases were not significantly changed from those obtained 2 days after sorting. These results suggest that CA-AhR affects cell cycle progression, especially in the G_1 phase.

The Inhibition of Growth by CA-AhR Is Mediated by Both XRE-dependent and -independent Mechanisms—To elucidate whether the inhibitory effect of CA-AhR on the growth of Jurkat T cells is mediated by an XRE-dependent or -independent mechanism, we generated an A78D mutant of the CA-AhR. The A78D mutant of wild-type AhR is translocated into the nucleus in the presence of TCDD and forms a heterodimer with ARNT. However, it lacks the potential for XRE-driven gene expression due to impaired XRE binding (24). To confirm that the disruption of transcription by A78D mutation is available for the CA-AhR, we examined the effects of A78D mutation introduced into the CA-AhR on localization and gene expression. When either CA-AhR-GFP or A78D mutant of CA-AhR-GFP (A78D-GFP) was transiently expressed in Jurkat T cells, a FACS analysis showed the same GFP expression patterns between both types of transfected cells, before and after sorting (Fig. 6*A*). Furthermore, the mRNA expression of CA-AhR-GFP or A78D-GFP was detected at the same level in both transfected cells by semiquantitative RT-PCR (Fig. 6*B*). The green fluorescence emitted by the GFP was mainly observed in the nuclear compartment in cells expressing A78D-GFP as well as CA-AhR-GFP (data not shown). However, as shown in Fig. 6*B*, only

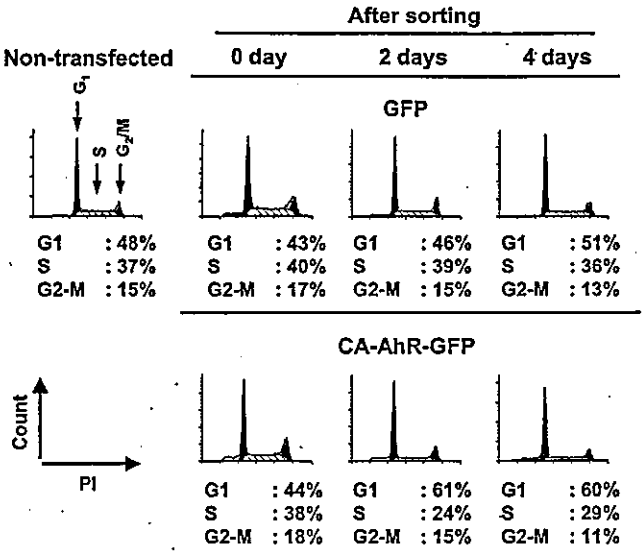

FIG. 5. **CA-AhR increases the percentage of cells in the G_1 phase.** The expression vector for either CA-AhR-GFP or GFP alone was transiently transfected into Jurkat T cells using DMRIE-C reagent. After 2 days, GFP-positive cells were sorted from the transfected cells using a FACSVantage SE and then cultured for the indicated time periods. The cells were stained with PI using a CycleTEST Plus DNA reagent kit, and DNA content was measured using a FACSCalibur. The percentages of cells in the G_1, S, and G_2/M phases were analyzed using ModFit software.

CA-AhR-GFP, but not A78D-GFP, induced CYP1A1 mRNA expression. These observations show that A78D-GFP is constitutively localized in the nucleus in the absence of TCDD, but it cannot induce gene expression by binding to the XRE.

Using these AhR mutants, the XRE dependence of the inhibitory effect of activated AhR was examined. As shown in Fig. 6*C*, CA-AhR markedly inhibited the increase in cell number (in agreement with the data shown in Fig. 2). On the other hand, the A78D mutant only partially inhibited the increase. This result indicates that both XRE-dependent and -independent mechanisms are involved in the CA-AhR-induced growth inhibition.

CA-AhR Induces Expression Changes of Genes Related to Apoptosis and Cell Cycle Arrest by an XRE-dependent Mechanism—Because CA-AhR induced apoptosis and the accumulation in the G_1 phase in Jurkat T cells, we examined whether CA-AhR changes the expression of genes related to apoptosis and cell cycle arrest and whether the regulations of these genes are mediated by XRE-dependent transcription. Two days after transfection, total RNA was isolated from the GFP-positive cells, and the gene expression was analyzed using an Affymetrix GeneChip. Genes related to apoptosis and cell cycle arrest were selected from the genes that showed at least a 2-fold change in gene expression in the cells expressing CA-AhR-GFP, as compared with cells expressing GFP alone, and their expression changes were confirmed by semiquantitative RT-PCR. Furthermore, we determined the relative -fold induction of each of the confirmed genes in cells expressing CA-AhR-GFP and in cells expressing A78D-GFP by a comparison with the cells expressing GFP alone (Fig. 7 and Table II). We found that CA-AhR up-regulates genes related to apoptosis (caspase 8, c-Jun, and Fas) (26, 27) and cell cycle arrest (cyclin G2, growth arrest and DNA-damage-inducible, alpha (GADD45A), $p21^{waf1}$, cell division autoantigen-1 (CDA1), and IL-9 receptor) (28–32). CA-AhR also up-regulated the genes involved in both apoptosis and cell cycle arrest (dual specificity phosphatase 6, GADD34, and TGF-β receptor II) (33–36). On the other hand, c-Myc, which plays an important role in the G_1/S transition

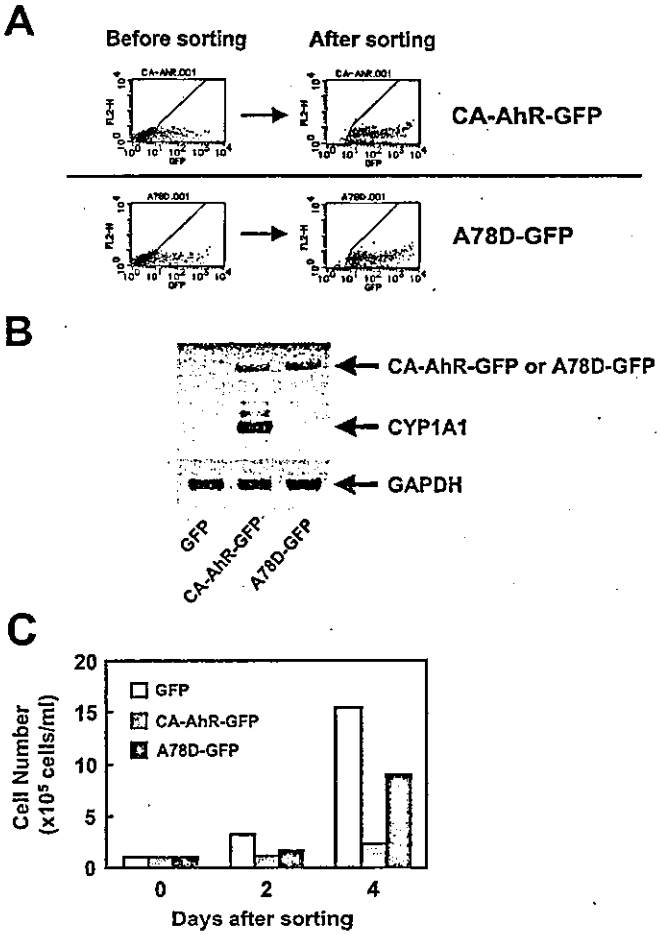

FIG. 6. **CA-AhR inhibits the growth of Jurkat T cells by the XRE-dependent and -independent mechanisms.** *A*, the expression vector for either CA-AhR-GFP, A78D-GFP, or GFP alone was transiently transfected into Jurkat T cells using DMRIE-C reagent. Two days after the transfection, GFP-positive cells were sorted using a FACSVantage SE. The GFP expression of the cells was analyzed before and after sorting, using a FACSCalibur. *B*, total RNA was isolated from the cells and mRNA expression levels of CYP1A1, CA-AhR-GFP, and glyceraldehyde-3-phosphate dehydrogenase were examined by semiquantitative RT-PCR. *C*, the sorted cells were cultured at 1×10^5 cells/ml, and the cell numbers at the indicated times were determined by trypan blue exclusion.

(37), was down-regulated in cells expressing CA-AhR-GFP. Furthermore, our results clarified that all the changes in these genes were dependent on transcription through the XRE, because only CA-AhR, but not A78D, induced expression changes of these genes (Fig. 7 and Table II).

DISCUSSION

In the present study, $CD4^+$ T cell line Jurkat T cells were transiently expressed with a CA-AhR, a model of ligand-activated AhR. We demonstrated that CA-AhR remarkably inhibits the growth of Jurkat T cells. We also clarified that CA-AhR induces both apoptosis and accumulation in the G_1 phase, which strongly suggests that these effects induce growth inhibition in Jurkat T cells. Furthermore, we showed that CA-AhR-induced growth inhibition is mediated by both XRE-dependent and -independent mechanisms, using an A78D mutant of the CA-AhR. With regard to the XRE-dependent mechanism, our results demonstrate that CA-AhR induces expression changes in genes related to apoptosis and cell cycle arrest. On the other hand, the XRE-independent growth inhibition, which is caused by the A78D mutant of the CA-AhR, may result from the interaction between CA-AhR and its target molecules. For in-

stance, it has been reported that RB specifically interacts with both an LXCXE motif in PAS B of the AhR and the C-terminal region of the AhR and that their direct interaction inhibits E2F-driven gene expression, leading to G_1 arrest (7, 8, 38). Although the CA-AhR protein lacks a PAS B region containing an LXCXE motif, it possesses the ability to specifically interact with RB through the C-terminal region. The semiquantitative RT-PCR data in our present and previous study (19) suggest that the CA-AhR was expressed in Jurkat T cells at a much higher level than the native AhR in mouse thymocytes and splenocytes. Therefore, we also cannot rule out the possibility that the XRE-independent growth inhibition was due to artifactual effects, such as stress response, of overexpression of the AhR protein in the nucleus. Further studies will be needed to elucidate the mechanism of XRE-independent growth inhibition.

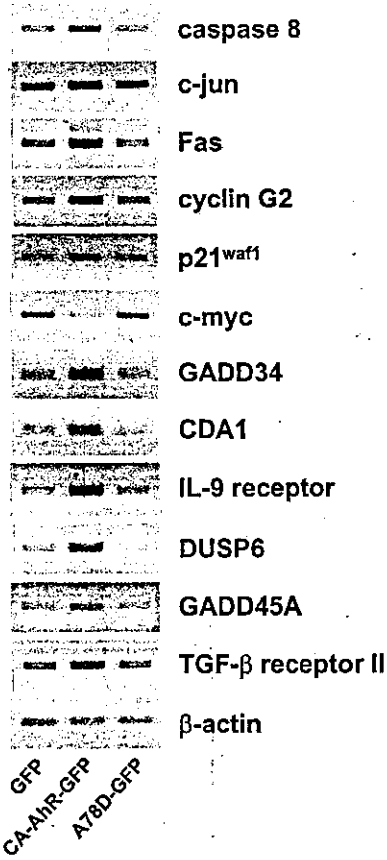

FIG. 7. **CA-AhR induces expression changes of genes related to apoptosis and cell cycle arrest by an XRE-dependent mechanism.** The expression vector for either CA-AhR-GFP, A78D-GFP, or GFP alone was transiently transfected into Jurkat T cells using DMRIE-C reagent. Two days after the transfection, GFP-positive cells were sorted using a FACSVantage SE. Total RNA was isolated from the cells, and gene expression was analyzed using an Affymetrix GeneChip. Genes related to apoptosis and cell cycle arrest were collected from the genes that showed at least a 2-fold change in gene expression in the cells expressing CA-AhR-GFP, as compared with the cells expressing GFP alone, and the expression changes of these genes were confirmed by semiquantitative RT-PCR.

The gene expression analysis suggests the involvement of several signaling pathways in the growth suppression of Jurkat T cells. The increase in Fas and caspase 8 transcripts by CA-AhR suggests that the Fas signaling pathway is involved in the CA-AhR-induced apoptosis. In agreement with our present data, previous studies using mice having a deficiency in the Fas signaling pathway have shown that TCDD decreases the cell number of anti-CD3-activated T cells through a Fas signaling pathway (39, 40). The study by Zeytun *et al.* (40) reported that Fas ligand was up-regulated in the spleen cells of mice exposed to TCDD. However, CA-AhR did not increase the expression level of Fas ligand in Jurkat T cells. This discrepancy between our study and that of Zeytun *et al.* suggests that TCDD-induced up-regulation of Fas ligand is due to the effect on non-T cells in spleen cells. As another apoptosis-related gene, we found that CA-AhR increases TGF-β receptor II transcript. The TGF-β signaling pathway has been reported to induce apoptosis and cell cycle arrest in T cells (36). Although CA-AhR induces no changes in the expression level of the TGF-β family (TGF-β1, β2, and β3) in Jurkat T cells (data not shown), the up-regulation of TGF-β receptor II by AhR activation in T cells may cause an increase in their susceptibility to TGF-β. CA-AhR also regulated a number of genes related to cell cycle arrest. We found that CA-AhR induces expression changes of genes involved not only in G_1 arrest (cyclin G2 and c-Myc) (28, 37) but also in G_2 arrest (GADD45A) (29), in both G_1 and G_2 arrest ($p21^{waf1}$) (30), and in multiphase cell cycle arrest (CDA1) (31). Through a cell cycle analysis, we showed that CA-AhR induced the accumulation in the G_1 phase by culturing for 2 days after sorting. However, further accumulation in the G_1 phase was not found by culturing for 4 days after sorting. These results may suggest

TABLE II

Relative-fold induction of CA-AhR-regulated genes in the XRE-dependent and -independent fashion

Gene expression changes by CA-AhR were examined by Affymetrix GeneChip analysis, and genes related to apoptosis and cell cycle arrest with at least two-fold changes in CA-AhR-GFP-transfected cells, as compared with GFP-alone transfected cells, were selected. Relative expression levels of the selected genes in cells expressing either CA-AhR-GFP or A78D-GFP were determined by semiquantitative RT-PCR.

Description	Change[a]	Functions	CA-AhR, change[b]	A78D, change[c]
			-fold	
Caspase 8	Up	Apoptosis	1.72	0.76
c-Jun	Up	Apoptosis	1.42	0.85
Fas	Up	Apoptosis	2.66	0.62
Cyclin G2	Up	G_1 arrest	2.20	0.78
c-Myc	Down	G_1/S transition	0.29	0.75
GADD45A	Up	G_2 arrest	1.30	0.71
$p21^{waf1}$	Up	G_1 arrest and G_2 arrest	1.98	1.19
CDA1	Up	Growth arrest	2.36	0.73
IL-9 receptor	Up	Growth arrest	4.79	1.33
DUSP6	Up	Apoptosis and growth arrest	3.00	0.57
GADD34	Up	Apoptosis and growth arrest	2.18	0.69
TGF-β receptor II	Up	Apoptosis and growth arrest	1.79	0.89

[a] Gene expression changes were determined by Affymetrix GeneChip analysis.

[b] Relative gene expression level was determined in cells expressing CA-AhR-GFP, as compared with cells expressing GFP alone, by semiquantitative RT-PCR.

[c] Relative gene expression level was determined in cells expressing A78D-GFP, as compared with cells expressing GFP alone, by semiquantitative RT-PCR.

that CA-AhR causes alteration of the G_1/S transition at an early stage and then inhibits cell cycle progression at various stages of the cell cycle.

With regard to how CA-AhR regulates the transcription of these genes, a search for the human genome sequences of the NCBI demonstrated that the 5′-flanking regions of GADD34, IL-9 receptor, CDA1, and c-Jun genes contain the core consensus sequence of XRE (5′-TNGCGTG-3′ or 5′-CACGCNA-3′), suggesting that these genes are directly regulated by activated AhR through the XRE, whereas other genes seem to be regulated by indirect mechanisms. The expression of Fas, GADD45A, $p21^{waf1}$, and caspase 8 are known to be up-regulated by the activation of p53 (41, 42). Recently, it has been reported that GADD34 induces phosphorylation of p53 and enhances $p21^{waf1}$ expression (35). Likewise, CA-AhR may up-regulate genes such as Fas, GADD45A, and caspase 8 through induction of GADD34 and following p53 activation. In addition, it has been reported that the induction of CYP1A1 causes DNA damage (43), probably leading to the activation of p53. Therefore, this p53-dependent pathway may be involved in CA-AhR-induced apoptosis and cell cycle arrest.

Previous studies have reported that TCDD induces apoptosis in AhR-null T cell clones, including Jurkat T cells, in an AhR-independent manner (20, 44). However, Jurkat T cells used in this study were not susceptible to apoptosis even in the presence of 10 nM TCDD (data not shown). Although the reason for the discrepancy is unclear, our results well indicate that activated AhR is essential for the inhibition of T cell growth by TCDD, in agreement with the findings that AhR expression is indispensable for TCDD-induced immunosuppression *in vivo* (10, 11).

In summary, we demonstrated that CA-AhR induces the growth inhibition of Jurkat T cells, with an increase in apoptosis and the accumulation of the cells in the G_1 phase. Furthermore, we showed that both XRE-dependent and -independent mechanisms are involved in CA-AhR-induced growth inhibition and that CA-AhR regulates the expression of several genes related to apoptosis and cell cycle arrest in an XRE-dependent manner. Further studies will aim to identify target gene(s) and protein(s) mainly responsible for the inhibition of T cell growth by the XRE-dependent and -independent mechanisms. $CD4^+$ helper T cells play an important role in both humoral and cellular immunity, where TCDD inhibited the increase in the number of $CD4^+$ T cells, following immunization (16, 45). The present data may provide a mechanism for the suppression of both humoral and cellular immunity.

Acknowledgments—We gratefully acknowledge Drs. Yoshihiro Miwa and Junko Tanaka (University of Tsukuba) for providing pEB6 expression vectors and technical advice on plasmid construction, and Kazuhiro Shiizaki (National Institute for Environmental Studies) for technical advice on point mutation in the AhR. We also thank Michiyo Matsumoto for their excellent technical and Kyoko Nakazawa for secretarial assistance.

REFERENCES

1. Birnbaum, L. S., and Tuomisto, J. (2000) *Food Addit. Contam.* **17,** 275–288
2. Tohyama, C. (2002) *Environ. Sci.* **9,** 37–50
3. Fernandez-Salguero, P. M., Hilbert, D. M., Rudikoff, S., Ward, J. M., and Gonzalez, F. J. (1996) *Toxicol. Appl. Pharmacol.* **140,** 173–179
4. Mimura, J., and Fujii-Kuriyama, Y. (2003) *Biochim. Biophys. Acta* **1619,** 263–268
5. Petrulis, J. R., and Perdew, G. H. (2002) *Chem. Biol. Interact.* **141,** 25–40
6. Whitlock, J. P., Jr. (1999) *Annu. Rev. Pharmacol. Toxicol.* **39,** 103–125
7. Puga, A., Barnes, S. J., Dalton, T. P., Chang, C. Y., Knudsen, E. S., and Maier, M. A. (2000) *J. Biol. Chem.* **275,** 2943–2950
8. Ge, N.-L., and Elferink, C. J. (1998) *J. Biol. Chem.* **273,** 22708–22713
9. Tian, Y., Ke, S., Denison, M. S., Rabson, A. B., and Gallo, M. A. (1999) *J. Biol. Chem.* **274,** 510–515
10. Vorderstrasse, B. A., Steppan, L. B., Silverstone, A. E., and Kerkvliet, N. I. (2001) *Toxicol. Appl. Pharmacol.* **171,** 157–164
11. Kerkvliet, N. I. (2002) *Int. Immunopharmacol.* **2,** 277–291
12. Laiosa, M. D., Wyman, A., Murante, F. G., Fiore, N. C., Staples, J. E., Gasiewicz, T. A., and Silverstone, A. E. (2003) *J. Immunol.* **171,** 4582–4591
13. Staples, J. E., Murante, F. G., Fiore, N. C., Gasiewicz, T. A., and Silverstone, A. E. (1998) *J. Immunol.* **160,** 3844–3854
14. Kerkvliet, N. I., Shepherd, D. M., and Baecher-Steppan, L. (2002) *Toxicol. Appl. Pharmacol.* **185,** 146–152
15. Holsapple, M. P., Snyder, N. K., Wood, S. C., and Morris, D. L. (1991) *Toxicology* **69,** 219–255
16. Ito, T., Inouye, K., Fujimaki, H., Tohyama, C., and Nohara, K. (2002) *Toxicol. Sci.* **70,** 46–54
17. Nohara, K., Fujimaki, H., Tsukumo, S., Inouye, K., Sone, H., and Tohyama, C. (2002) *Toxicology* **172,** 49–58
18. Fujimaki, H., Nohara, K., Kobayashi, T., Suzuki, K., Eguchi-Kasai, K., Tsukumo, S., Kijima, M., and Tohyama, C. (2002) *Toxicol. Sci.* **66,** 117–124
19. Doi, H., Baba, T., Tohyama, T., and Nohara, K. (2003) *Chemosphere* **52,** 655–662
20. Hossain, A., Tsuchiya, S., Minegishi, M., Osada, M., Ikawa, S., Tezuka, F., Kaji, M., Konno, T., Watanabe, M., and Kikuchi, H. (1998) *J. Biol. Chem.* **273,** 19853–19858
21. Lawrence, P., Leid, M., and Kerkvliet, N. I. (1996) *Toxicol. Appl. Pharmacol.* **138,** 275–284
22. McGuire, J., Okamoto, K., Whitelaw, M. L., Tanaka, H., and Poellinger, L. (2001) *J. Biol. Chem.* **276,** 41841–41849
23. Köhle, C., Hassepass, I., Bock-Hennig, B. S., Bock, K. W., Poellinger, L., and McGuire, J. (2002) *Arch. Biochem. Biophys.* **402,** 172–179
24. Levine, S. L., Petrulis, J. R., Dubil, A., and Perdew, G. H. (2000) *Mol. Pharmacol.* **58,** 1517–1524
25. Tanaka, J., Miwa, Y., Miyoshi, K., Ueno, A., and Inoue, H. (1999) *Biochem. Biophys. Res. Commun.* **264,** 938–943
26. Peter, M. E., and Krammer, P. H. (1998) *Curr. Opin. Immunol.* **10,** 545–551
27. Leppä, S., and Bohmann, D. (1999) *Oncogene* **18,** 6158–6162
28. Bennin, D. A., Don, A. S. A., Brake, T., McKenzie, J. L., Rosenbaum, H., Ortiz, L., DePaoli-Roach, A. A., and Horne, M. C. (2002) *J. Biol. Chem.* **277,** 27449–27467
29. Wang, X. W., Zhan, Q., Coursen, J. D., Khan, M. A., Konthy, H. U., Yu, L., Hollander, M. C., O'Connor, P. M., Fornace, A. J., Jr., and Harris, C. C. (1999) *Proc. Natl. Acad. Sci. U. S. A.* **96,** 3706–3711
30. Medema, R. H., Klompmaker, R., Smits, V. A., and Rijksen, G. (1998) *Oncogene* **16,** 431–441
31. Chai, Z., Sarcevic, B., Mawson, A., and Toh, B. H. (2001) *J. Biol. Chem.* **276,** 33665–33674
32. Demoulin, J. B., Van Snick, J., and Renauld, J. C. (2001) *Cell Growth Differ.* **12,** 169–174
33. Furukawa, T., Sunamura, M., Motoi, F., Matsuno, S., and Horii, A. (2003) *Am. J. Pathol.* **162,** 1807–1815
34. Hollander, M. C., Sheikn, M. S., Yu, K., Zhan, Q., Iglesias, M., Woodworth, C., and Fornace, A. J., Jr. (2001) *Int. J. Cancer* **96,** 22–31
35. Yagi, A., Hasegawa, Y., Xiao, H., Haneda, M., Kojima, E., Nishikimi, A., Hasegawa, T., Shimokata, K., and Isobe, K. (2003) *J. Cell. Biochem.* **90,** 1242–1249
36. Gorelik, L., and Flavell, R. A. (2002) *Nat. Rev. Immunol.* **2,** 46–53
37. Schorl, C., and Sedivy, J. M. (2003) *Mol. Biol. Cell* **14,** 823–835
38. Elferink, C. J., Ge, N.-L., and Levine, A. (2001) *Mol. Pharmacol.* **59,** 664–673
39. Dearstyne, E. A., and Kerkvliet, N. I. (2002) *Toxicology* **170,** 139–151
40. Zeytun, A., McKallip, R. J., Fisher, M., Camacho, I., Nagarkatti, M., and Nagarkatti, P. S. (2002) *Toxicology* **178,** 241–260
41. Vogelstein, B., Lane, D., and Levine, A. J. (2000) *Nature* **408,** 307–310
42. Liedtke, C., Gröger, N., Manns, M. P., and Trautwein, C. (2003) *J. Biol. Chem.* **278,** 27593–27604
43. Park, J.-Y. K., Shigenaga, M. K., and Ames, B. N. (1996) *Proc. Natl. Acad. Sci. U. S. A.* **93,** 2322–2327
44. Park, J. H., Hahn, E. J., Kong, J. H., Cho, H. J., Yoon, C. S., Cheong, S. W., Oh, G. S., and Youn, H. J. (2003) *Toxicol. Lett.* **145,** 55–68
45. Kerkvliet, N. I., Steppan, L. B., Shepherd, D. M., Oughton, J. A., Vorderstrasse, B. A., and DeKrey, G. K. (1996) *J. Immunol.* **157,** 2310–2319

Activation of Hepatic Nrf2 *In Vivo* by Acetaminophen in CD-1 Mice

Christopher E. P. Goldring,[1] Neil R. Kitteringham,[1] Robert Elsby,[1] Laura E. Randle,[1] Yuri N. Clement,[2] Dominic P. Williams,[1] Michael McMahon,[3] John D. Hayes,[3] Ken Itoh,[4] Masayuki Yamamoto,[4] and B. Kevin Park[1]

The transcription factor NF-E2-related factor 2 (Nrf2) plays an essential role in the mammalian response to chemical and oxidative stress through induction of hepatic phase II detoxification enzymes and regulation of glutathione (GSH). Enhanced liver damage in Nrf2-deficient mice treated with acetaminophen suggests a critical role for Nrf2; however, direct evidence for Nrf2 activation following acetaminophen exposure was previously lacking. We show that acetaminophen can initiate nuclear translocation of Nrf2 *in vivo*, with maximum levels reached after 1 hour, in a dose dependent manner, at doses below those causing overt liver damage. Furthermore, Nrf2 was shown to be functionally active, as assessed by the induction of epoxide hydrolase, heme oxygenase-1, and glutamate cysteine ligase gene expression. Increased nuclear Nrf2 was found to be associated with depletion of hepatic GSH. Activation of Nrf2 is considered to involve dissociation from a cytoplasmic inhibitor, Kelch-like ECH-associated protein 1 (Keap1), through a redox-sensitive mechanism involving either GSH depletion or direct chemical interaction through Michael addition. To investigate acetaminophen-induced Nrf2 activation we compared the actions of 2 other GSH depleters, diethyl maleate (DEM) and buthionine sulphoximine (BSO), only 1 of which (DEM) can function as a Michael acceptor. For each compound, greater than 60% depletion of GSH was achieved; however, in the case of BSO, this depletion did not cause nuclear translocation of Nrf2. In conclusion, GSH depletion alone is insufficient for Nrf2 activation: a more direct interaction is required, possibly involving chemical modification of Nrf2 or Keap1, which is facilitated by the prior loss of GSH. (HEPATOLOGY 2004;39:1267–1276.)

The cellular defense response to chemical or oxidative stress is characterized by a coordinated induction of phase II drug-metabolizing enzymes and glutathione (GSH) synthesis, which protect the cell through the elimination of electrophiles and reactive oxygen species (ROS).[1,2] Central to this transcriptional response is a common DNA sequence found within the promoter regions of these phase II genes, which is referred to as the antioxidant (or electrophile) responsive element (ARE/EpRE).[3,4]

The ARE, first identified in the upstream regulatory region of the rat *GSTA2* gene,[5] was found to respond to oxidative stress.[6] The resemblance of the consensus ARE to the DNA *cis* element recognized by nuclear factor-erythroid 2 (NF-E2),[7] aligned with the discovery of a subset of basic leucine zipper (bZip) transcription factors known as the cap 'n' collar proteins that presently comprise the NF-E2-related factors 1, 2, and 3 (Nrf1, Nrf2, and Nrf3), and Bach1 and Bach2, revealed a family of ARE-interacting factors. Studies using forced expression of Nrf2 have demonstrated this bZip protein to be a functionally critical component for ARE activation.[8–11] Gene deletion studies have also shed light on the importance of Nrf2 in driving the antioxidant transcriptional response.[12–15]

Under normal homeostatic conditions, Nrf2 is believed to reside predominantly within the cytoplasm of the cell. Activation of Nrf2, which initially depends on its nuclear translocation, has been postulated to occur through a number of signal transduction pathways (for a

Abbreviations: GSH, reduced glutathione; ROS, reactive oxygen species; ARE/EpRE, antioxidant/electrophile response element; NF-E2, nuclear factor-erythroid 2; bZip, basic zipper protein; Nrf, NF-E2-related factor; Keap1, Kelch-like ECH-associated protein 1; NAPQI, N-acetyl-p-benzoquinoneimine; IP, intraperitoneal; DEM, diethyl maleate; BSO, buthionine sulfoximine; TBS, Tris-buffered saline; ALT, alanine transaminase; HO-1, heme oxygenase-1; GCLC, glutamate cysteine ligase catalytic subunit; mEH, microsomal epoxide hydrolase; mRNA, messenger RNA.

From the [1]Department of Pharmacology and Therapeutics, University of Liverpool, Liverpool, Merseyside, UK; [2]Pharmacology Unit, Faculty of Medical Sciences, University of the West Indies, St. Augustine, Trinidad and Tobago; [3]Biomedical Research Centre, University of Dundee, Dundee, Scotland; and [4]Center for Tsukuba Advanced Research Alliance, University of Tsukuba, Tsukuba, Japan.

Received September 26, 2003; accepted January 13, 2004.

Supported by the Wellcome Trust.

B.K.P. is a Wellcome Principal Research Fellow at the University of Liverpool. Y.N.C. was a Wellcome Travelling Fellow at the University of Liverpool.

Address reprint requests to: Professor Kevin Park, Department of Pharmacology and Therapeutics, University of Liverpool, Sherrington Buildings, Ashton Street, Liverpool, L69 3GE, Merseyside, UK. E-mail: B.K.Park@liv.ac.uk; fax: 0044-0-151-794-5540.

Published online in Wiley InterScience (www.interscience.wiley.com).

DOI 10.1002/hep.20183

review, see Kong et al.[16]). Intriguingly, it has been shown that Nrf2 is prevented from accessing the nucleus through tethering to an inhibitor protein, Kelch-like ECH-associated protein 1 (Keap1).[17,18] Recent work has shown that the inhibitory mechanism is probably via the ability of Keap1 to direct Nrf2 for proteosome-mediated degradation under conditions of normal cellular homeostasis.[19-21] Although the triggering mechanism for the uncoupling event is not known, it has been postulated to depend on 1 or more reactive thiol groups in the Keap1 molecule.[17] Since all ARE inducers react with sulfhydryl groups, it has been suggested that Keap1 could be a candidate cellular xenobiotic sensor/trigger.[22]

Acetaminophen (paracetamol) is a human hepatotoxin at high doses and is still associated with several hundred deaths a year in both the United States[23] and the United Kingdom.[24] At therapeutic doses, toxicity is an extremely rare event. Despite over 30 years of research into its mechanism of toxicity, the precise biochemical basis remains unknown.[25] The role of metabolic activation in acetaminophen hepatotoxicity has been confirmed by studies with cytochrome P450 knockout mice,[26,27] and it has been proposed that an electrophilic species, N-acetyl-*p*-benzoquinoneimine (NAPQI), underlies the tissue damage observed. NAPQI can react directly with protein and nonprotein thiols, and GSH depletion is a hallmark of acetaminophen poisoning.[28] This process occurs remarkably rapidly with protein adducts being detectable in mouse liver within 15 minutes of an intraperitoneal (IP) dose of acetaminophen.[29] Furthermore, the formation of NAPQI may be associated with the generation of ROS and oxidative stress, and this has been suggested as a primary cause of the liver damage,[30-32] although several other mechanisms have also been implicated. Depressed mitochondrial function aggravated by the formation of peroxynitrite from superoxide and nitric oxide, together with disrupted calcium homeostasis are also believed to be involved in acetaminophen-induced liver injury (for reviews, see Cohen et al.[31] and Jaeschke et al.[32]). Two independent studies with gene knockout mice have shown that acetaminophen hepatotoxicity is exacerbated in the absence of Nrf2,[14,33] suggesting that the antioxidant response is activated by exposure to acetaminophen and affords protection. However, it has not yet been demonstrated whether acetaminophen treatment *in vivo* actually results in Nrf2 activation. Here we report that administration of acetaminophen to mice does indeed result in increased nuclear levels of Nrf2 in the liver, consistent with a pronounced nuclear translocation of Nrf2 from the cytoplasm. Furthermore, we have investigated the functionality of Nrf2 activation by demonstrating increased expression of several downstream Nrf2 target genes.

Materials and Methods

All chemicals were purchased from Sigma (Poole, UK) unless otherwise stated.

Animals were obtained from Charles River (Margate, UK). All experiments were undertaken in accordance with criteria outlined in a license granted under the Animals (Scientific Procedures) Act of 1986 and approved by the Animal Ethics Committee of the University of Liverpool.

Dosing Regime. Nonfasted animals were dosed as described previously.[34] Briefly, male CD-1 mice (25 - 35 g) were administered a single IP dose of acetaminophen (50, 150, 300, 530, 700, and 1000 mg/kg in 0.9% saline), diethyl maleate (DEM; 2.35, 4.7, and 7.05 mmol/kg, administered in corn oil), or buthionine sulfoximine (BSO; 7.2 mmol/kg in 0.9% saline). Untreated animals or animals treated with vehicle alone were used as controls. Various concentrations of acetaminophen in saline (15 mg/mL for the 50 and 150 mg/kg doses and 30 mg/mL for the 300, 530, 700, and 1000 mg/kg doses), DEM in corn oil (0.622 mol for each of the doses) and BSO in saline (1 mol) were prepared. The volumes injected in the acetaminophen studies varied from 100 μL to 1000 μL, and an equal volume of saline was injected into each of the vehicle control groups. For the DEM studies, 100 μL to 300 μL of DEM in corn oil was injected; 100 μL of corn oil was injected into the vehicle control mice. For the BSO study, equal volumes of saline or BSO in saline (approx 200 μL) were injected into the mice. At various time points after dosing, the animals were killed by cervical dislocation and the livers were removed immediately and rinsed in 0.9% saline.

Determination of Serum Alanine Transaminase Levels. Blood was collected 5 hours (acetaminophen treatment) or 24 hours (DEM treatment) after treatment by cardiac puncture from a satellite group of 2 animals (acetaminophen treatment) or 4 animals (DEM treatment) included with each of the doses investigated. The blood was stored at 4°C and allowed to clot overnight prior to isolation of serum. Serum alanine transaminase (ALT) levels were determined using ThermoTrace Infinity ALT Liquid stable reagent (Alpha Labs, Eastleigh, UK), according to the manufacturer's instructions. Hepatotoxicity was considered to be indicated at levels of ALT greater than 200 IU/L, which in our experience are associated with whole organ manifestations of toxicity.

Determination of Hepatic Reduced GSH Levels. Hepatic GSH was determined using a microtiter plate assay according to the method of Vandeputte et al.[35] The GSH levels were calculated by subtracting the amount of glutathione disulfide from the amount of total GSH in each sample.

Nuclear Extractions. Mouse hepatic nuclear protein extractions were carried out on fresh, homogenized tissue, using the classical Dignam procedure, as described previously,[36,37] with the exception of the nuclear extracts prepared from the acetaminophen- and BSO-treated mice used for Western analysis. For these samples, the whole nuclei prepared by the conventional centrifugation steps as outlined in the Dignam method were solubilized at 4°C for 10 minutes in a radio-immunoprecipitation assay (RIPA) buffer (Dignam lysis buffer containing 1% sodium deoxycholate and 0.1% sodium dodecyl sulfate (SDS) (wt/vol)) and centrifuged at 14,000*g* for 10 minutes at 4°C. The supernatants were removed and stored at −80°C prior to analysis. Separate extracts were prepared using the conventional (Dignam) 0.35 mol NaCl nuclear protein extraction for the DEM-treated samples.

Western Analysis. Hepatic Nrf2 nuclear translocation was determined by Western blot analysis. Briefly, nuclear extracts (25 μg of protein) were separated by denaturing electrophoresis on premade 10% or 12% Nupage Novex Bis-Tris gels (Invitrogen, Paisley, UK) using 3-(N-Morpholino) propane sulfonic acid (MOPS)-SDS running buffer and subsequently transferred to nitrocellulose membranes. After incubation in blocking buffer (10% fat-free milk in Tris-buffered saline (TBS, pH 7) containing 1% Tween 20) for 0.5 hours, membranes were incubated with a rabbit anti-Nrf2 antiserum[21] at 1:4000 in TBS-Tween containing 2% milk for 1 hour. To ensure equal loading and transfer in the Western analysis of nuclear extracts, membranes were routinely stained using Ponceau Red. Following multiple washes with TBS-Tween, the secondary antibody was added (peroxidase-conjugated goat anti-rabbit immunoglobulin G; 1:4000 in TBS-Tween containing 2% milk). Visualization of the protein-antibody conjugate was performed using enhanced chemiluminescence, and band volumes were quantified by UVISoft software (UVITech, Cambridge, UK).

Northern Analysis. Heme oxygenase-1 (HO-1), glutamate cysteine ligase catalytic subunit (GCLC), and microsomal epoxide hydrolase (mEH) messenger RNA (mRNA) levels were determined by conventional Northern blot analysis. The 18S ribosomal RNA band was used as the internal control.

Statistical Analysis. Results are expressed as mean ± standard deviation. All values to be compared were analyzed for nonnormality using the Shapiro-Wilk test and for equivalence of variance between groups with the F test. Student's unpaired *t* test was used where parametric analysis was indicated; otherwise, the Mann-Whitney test was used. Results were considered significant when *P* values were less than .05.

Results

***Acetaminophen Administration Triggers Nrf2 Nuclear Translocation* In Vivo.** Activation of Nrf2 was determined by Western analysis of nuclear extracts from liver homogenate prepared from CD-1 mice treated with a range of acetaminophen doses. Acetaminophen resulted in a pronounced increase in nuclear Nrf2, consistent with enhanced nuclear translocation. Ideally, this translocation would be monitored as the appearance of the Nrf2 protein in the nuclei concomitant with a decrease in the protein in the cytosol. In fact, we were unable to detect Nrf2 in liver cytosolic fractions from any of the control or treated animals. This is not unexpected given that Nrf2 is known to be constitutively degraded prior to activation, at which point the protein migrates to the nucleus.[19-21] Furthermore, we have ruled out the possibility that the chemicals tested in this study might interact with the Nrf2 protein to enhance its immunogenicity in our assay by incubating rNrf2 with NAPQI (the reactive metabolite of acetaminophen) and DEM *in vitro*: the Nrf2 signal did not change after treatment (data not shown). Fig. 1A shows a representative Western blot of nuclear extracts obtained from animals treated with 700 mg/kg acetaminophen and vehicle controls. The induced Nrf2 protein is identified in the treated nuclei by the inclusion of a co-migrating mouse Nrf2 positive control. Nrf2 positive control was also spiked into several putative Nrf2-induced nuclear extracts to confirm the probable identity of the induced band (data not shown). The nonspecific bands were revealed as abundant liver proteins by the use of Ponceau Red staining. Nrf2 nuclear translocation was observed in each of the 5 treated animals compared to the vehicle-treated controls at and above a dose of 150 mg/kg acetaminophen (Fig. 1B). This occurred at each of the doses within 60 minutes after acetaminophen administration. Only low levels of nuclear Nrf2 were detected in the control animals from any of the treatment groups.

Translocation of Nrf2 was not obviously associated with the toxicity of the acetaminophen dose, at least as assessed by plasma ALT levels (Fig. 1B), where we have assumed hepatotoxicity at ALT values above 200 IU/L in our 5-hour satellite treatment groups. In our experience, ALT levels above 200 IU/L are associated with severe overt toxicity. Nuclear Nrf2 was increased above control levels at both nontoxic and toxic doses, although nuclear Nrf2 levels were highest at the 2 most toxic doses.

To define the relationship between the extent of Nrf2 nuclear translocation and the dose of acetaminophen, we pooled the 5 nuclear extracts obtained at each dose and

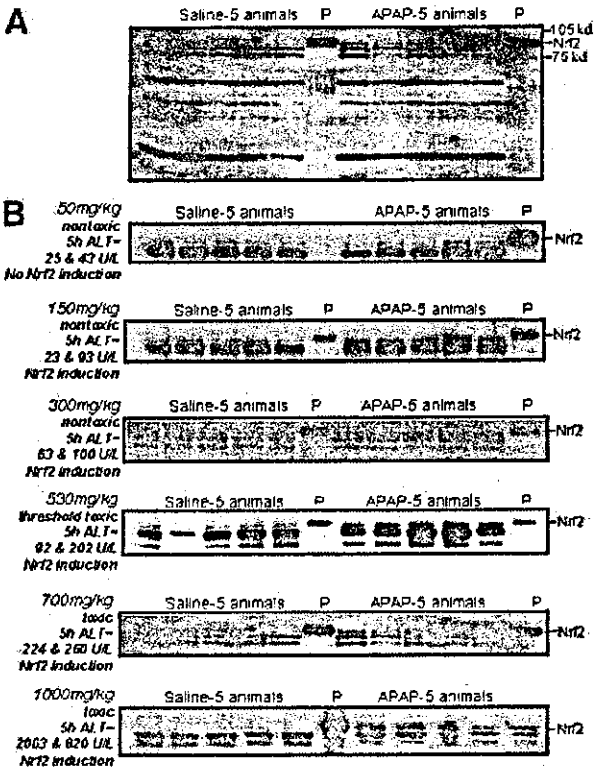

Fig. 1. Acetaminophen induces nuclear translocation of Nrf2 independently of hepatotoxicity. Acetaminophen, or saline vehicle alone, was administered IP to CD-1 mice. After 60 minutes, animals were killed and whole liver nuclei prepared, washed, and extracted. Extracts (25 μg) representing liver nuclear proteins obtained from individual animals were separated by electrophoresis, alongside a mouse Nrf2-transfected 293T cell extract positive control (P) and analyzed by Western blotting. (A) A representative gel showing Nrf2 translocation at 700 mg/kg is shown in full. (B) A close-up image of the gel in the region around the correct migration of Nrf2 is shown at each dose. Each of the analyses was performed at least twice and yielded similar results. The toxicity of each of the doses of acetaminophen is also shown, as assessed by an ALT toxicity assay, carried out on a satellite group of 2 animals per treatment, 5 hours after dosing. APAP, acetaminophen.

subjected these to Western analysis (Fig. 2A). The means of data from 3 separate analyses were then plotted against the treatment dose of acetaminophen. The error bars represent the SD obtained within each of the treatment groups in the analyses shown in Fig. 1B and therefore are representative of the interanimal variation in nuclear Nrf2. The amount of Nrf2 present in the nuclear fraction was found to be linearly associated ($P < .0001$) with the dose of acetaminophen administered, from nontoxic through to toxic doses (Fig. 2B).

***Diethyl Maleate Administration Triggers Nrf2 Nuclear Translocation* In Vivo.** The direct relationship between dose and nuclear Nrf2 obtained with acetaminophen indicated that hepatotoxicity as assessed by ALT determination was not required to cause Nrf2 activation *in vivo*. To confirm this observation, we employed the model compound DEM, which is equally as effective as acetaminophen in depleting GSH but lacks its ability to elicit elevated serum transaminases, indicative of liver damage, at the doses used in this study. Treatment of mice with DEM for 60 minutes resulted in hepatic Nrf2 nuclear translocation (Fig. 3A). This translocation was significantly different from corn oil control values at the 4.7 mmol/kg (236 ± 31% of corn oil controls; $P < .0005$) and 7.05 mmol/kg (652 ± 55% of corn oil controls; $P < .0001$) doses of DEM. No toxicity was seen at any of the doses of DEM used, as judged by the 24-hour ALT data (ALT data: 2.35 mmol/kg = 28 ± 21 U/L; 4.7 mmol/kg = 26 ± 17 U/L; 7.05 mmol/kg = 17 ± 5.7 U/L).

Acetaminophen and Diethyl Maleate Treatment Induces Maximal Nuclear Nrf2 Levels 60 Minutes After Treatment. In order to understand better the nature of the nuclear Nrf2 response to acetaminophen and DEM, we carried out time course studies over a 48-hour period. Both treatments elicited significantly increased levels of nuclear Nrf2 after just 30 minutes (Fig. 4), maximum levels being attained after approximately 1 hour. Thereafter, nuclear Nrf2 levels dropped in both treatments. Nrf2 had returned to control levels between 2 hours and 24 hours after treatment with DEM; this process was slower in the acetaminophen-treated mice, in which baseline levels were reached after approximately 48 hours.

Nrf2 Nuclear Translocation* In Vivo *Is Functionally Relevant as Assessed by Northern Blotting of Nrf2-Dependent Genes. Messenger RNA levels of 3 genes, HO-1, GCLC, and mEH, known to be transcriptionally dependent on Nrf2,[9,10] were analyzed in livers of mice treated with acetaminophen or DEM. At a dose of 530 mg/kg of acetaminophen, at which we observed an approximately 4-fold increase in nuclear Nrf2 (Fig. 2), mRNA levels of *mEH, GCLC*, and *HO-1* were significantly increased 60 minutes after drug administration compared with vehicle-treated controls (Fig. 5A). This confirms that the Nrf2 translocation observed was functionally significant. We also assessed the effect of translocation of Nrf2, at the highest and lowest doses of acetaminophen that affected nuclear accumulation of the bZip protein, on the expression of these genes. Interestingly, at the 150 mg/kg dose, which was the lowest dose that promoted Nrf2 translocation, only the HO-1 mRNA was significantly increased (Fig. 5B). At the 1,000 kg dose, there were no significant differences between the treated and control groups in the mRNA expression of HO-1, GCLC, or mEH (Fig. 5C). We also assessed these genes after administration of 7.05 mmol/kg DEM to check that the effects we observed with acetaminophen were not

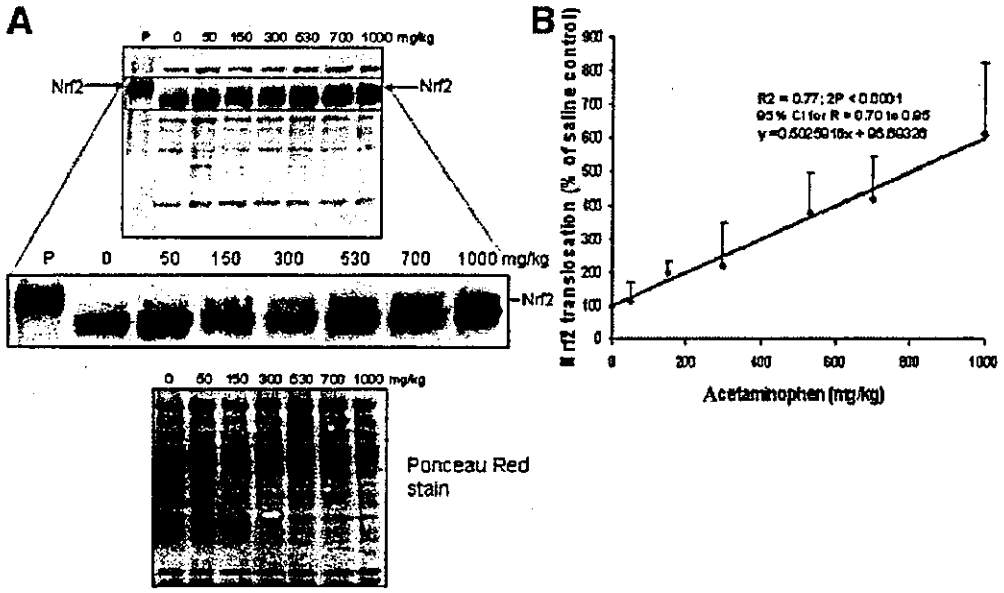

Fig. 2. Acetaminophen induces Nrf2 nuclear translocation *in vivo* in a linear fashion. Acetaminophen, or saline vehicle alone, was administered IP to CD-1 mice. After 60 minutes, animals were killed and whole liver nuclei prepared, washed, and extracted. Extracts (25 μg) were pooled and separated by electrophoresis as described in Fig 1. The analysis was performed 3 times. (A) **(top)** A representative gel is shown. Membranes probed for Nrf2 by Western blotting were always reversibly stained using Ponceau Red stain prior to blocking and antibody probing. This ensured equal loading of total nuclear protein onto each gel and provided a means for monitoring the integrity of the nuclear extracts from each of the treatment groups. A typical stained membrane is shown and is identical to the membrane probed for Nrf2. The staining shows little difference between the treatment groups with respect to the pattern of abundant nuclear proteins detectable using this technique. The gels were densitometrically scanned, and the amount of nuclear Nrf2 was determined as a percentage of the vehicle-treated animals. (B) The means of these determinations were then plotted against the dose of acetaminophen administered. The **error bars** represent the SD of the data (n = 5) for each of the treatment groups as calculated from the densitometry of Nrf2 in each of the nuclear extracts from each group in discrete Western analyses, as shown in Fig. 1B. SD values have been normalized to each of the data points to give an estimate of the interanimal variation within each group.

chemical-specific. In fact, the mRNAs of 2 of these genes, *HO-1* and *GCLC*, were numerically increased upon DEM treatment (Fig. 5D), suggesting that the Nrf2 translocation observed with DEM is also functionally significant.

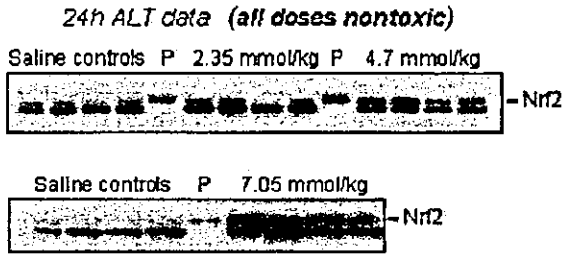

Fig. 3. Nontoxic doses of diethyl maleate (DEM) induce Nrf2 nuclear translocation *in vivo*. DEM, with time-matched controls, was administered IP to CD-1 mice (n = 4 for each dose plus controls). After 60 minutes, animals were killed and whole liver nuclei prepared, washed, and extracted. Extracts (25 μg) representing liver nuclear proteins obtained from individual animals were separated by electrophoresis, alongside a mouse Nrf2-transfected 293T cell extract positive control (P), and analyzed by Western blotting. The analyses were performed twice, and representative gels are shown here. The gels were densitometrically scanned, and the amount of nuclear Nrf2 was determined as a percentage of the time-matched control animals.

Translocation of Nrf2 to the Nucleus Is Associated With Levels of Hepatic GSH but Also Requires Chemical Modification of Sensor Protein(s). Since both acetaminophen and DEM are known to deplete GSH, the primary antioxidant in the liver, the relationship between hepatic GSH and Nrf2 nuclear translocation was investigated. We measured hepatic GSH at each of the doses of acetaminophen and DEM used to investigate translocation, 60 minutes after administration. Fig. 6A shows that nuclear Nrf2 translocation may be associated with GSH for both acetaminophen and DEM treatment; however, the nature of the relationship appears to be nonlinear.

The relationship between Nrf2 nuclear translocation and GSH depletion was also expressed relative to the dose of acetaminophen administered. As shown in Fig. 6B, a small increase in Nrf2 translocation is seen when GSH is depleted to 30% of its initial level. This increase is much more dramatic when GSH falls below 30%.

Finally, the association between Nrf2 activation and GSH levels was further investigated using another GSH-depleting agent, BSO. BSO inhibits GCLC, the rate-limiting enzyme in GSH synthesis, leading to a fall in hepatic GSH, but it does not possess the α,β-unsaturated ketone

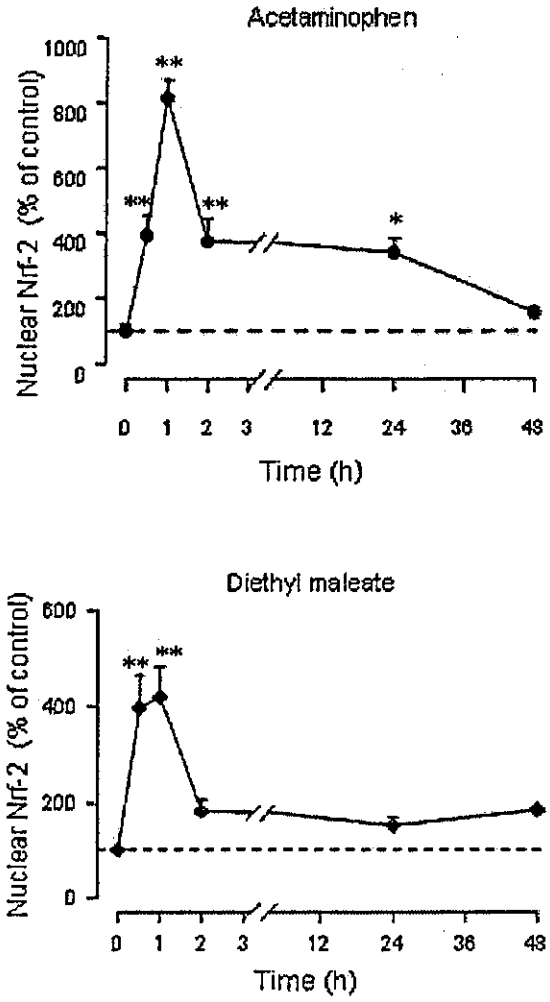

Fig. 4. Acetaminophen and diethyl maleate (DEM) treatment *in vivo* elicits enhanced hepatic nuclear Nrf2 within 30 minutes. Acetaminophen (530mg/kg in saline) and DEM (4.7 mmol/kg in corn oil) were administered IP to CD-1 mice (n = 3 or 4 for each time point). After the time points indicated, the animals were killed and whole liver nuclei prepared, washed, and extracted. Extracts (25 μg) representing liver nuclear proteins obtained from individual animals were separated by electrophoresis and analyzed by Western blotting. Each analysis was performed twice. Membranes were routinely verified for equal sample loading and equal transfer efficiency by using Ponceau Red staining. In all cases, values are the means ± SD of a representative experiment from duplicate determinations. For all data, values are expressed as a percentage of the zero time-point control value, indicated by the **broken line**. Statistical significance was assigned relative to untreated control animals as defined in Materials and Methods. $^*P < .05$; $^{**}P < .01$.

motif characteristic of a functional Michael acceptor, and is thus unable to modify proteins chemically, as is the case for acetaminophen and DEM. Treatment of mice (n = 5) with BSO for 1 and 2 hours resulted in 60% and 56% depletion in hepatic GSH, respectively. When we assayed levels of hepatic nuclear translocation of Nrf2 in these animals, no increase in either of the sets of BSO-treated animals was observed compared to the time-matched control group (data not shown). It therefore appears that, although Nrf2 activation is probably associated with GSH depletion, this alone is insufficient to trigger the event.

Discussion

The central and critical role played by Nrf2 in coordinating the mammalian cellular defense response to a variety of noxious and potentially harmful stimuli has become increasing well established over the last 10 years. It is now widely accepted that the redox sensitive regulation of this bZip transcription factor represents a convergence point for multiple stress-activated signaling pathways and results in the coordinated up-regulation of a battery of antioxidant proteins involved in cellular defense.[2,38] The involvement of Nrf2 in defense against chemical-induced stress is largely based on *in vitro* studies in cell lines, in which nuclear translocation has been clearly demonstrated following exposure to a variety of chemicals, including tertiary butyl hydroquinone,[39] butylated hydroxy anisole,[40] and DEM,[41] though not to acetaminophen. In contrast, there is a paucity of data demonstrating chemically induced Nrf2 activation *in vivo*. To our knowledge, the only documented evidence for Nrf2 translocation *in vivo* is that describing mouse hepatic nuclear Nrf2 after treatment with 3H-1,2-dithiole-3-thione[42] and a related compound, oltipraz.[43] Thus, the clear demonstration in the current study that acetaminophen administration to mice elicits a pronounced elevation of nuclear Nrf2 levels represents direct evidence for such activation in either an *in vivo* or an *in vitro* model system. Moreover, these data indicate that the nuclear translocation of Nrf2 *in vivo* is associated with levels of GSH, and thus the redox status, but is also dependent on the presence of chemical species with inherent protein reactivity. This follows from the observation that although acetaminophen, DEM, and BSO all depleted GSH to a similar extent, only DEM (a Michael acceptor) and acetaminophen (which is converted to the Michael acceptor NAPQI) elicited a rise in nuclear Nrf2.

The functional significance of the rise in nuclear Nrf2 was investigated by Northern analysis of 3 unrelated genes that have previously been characterized as downstream targets for Nrf2. Transcription of all 3 genes, HO-1, *GCLC*, and *mEH*, was enhanced in line with Nrf2 activation; however, there appeared to be different threshold levels of nuclear Nrf2 required for transcriptional activation in each case. Thus, there was a hierarchical order of induction, with *HO-1* being the only gene induced at the nontoxic 150 mg/kg dose, while all 3 genes were induced

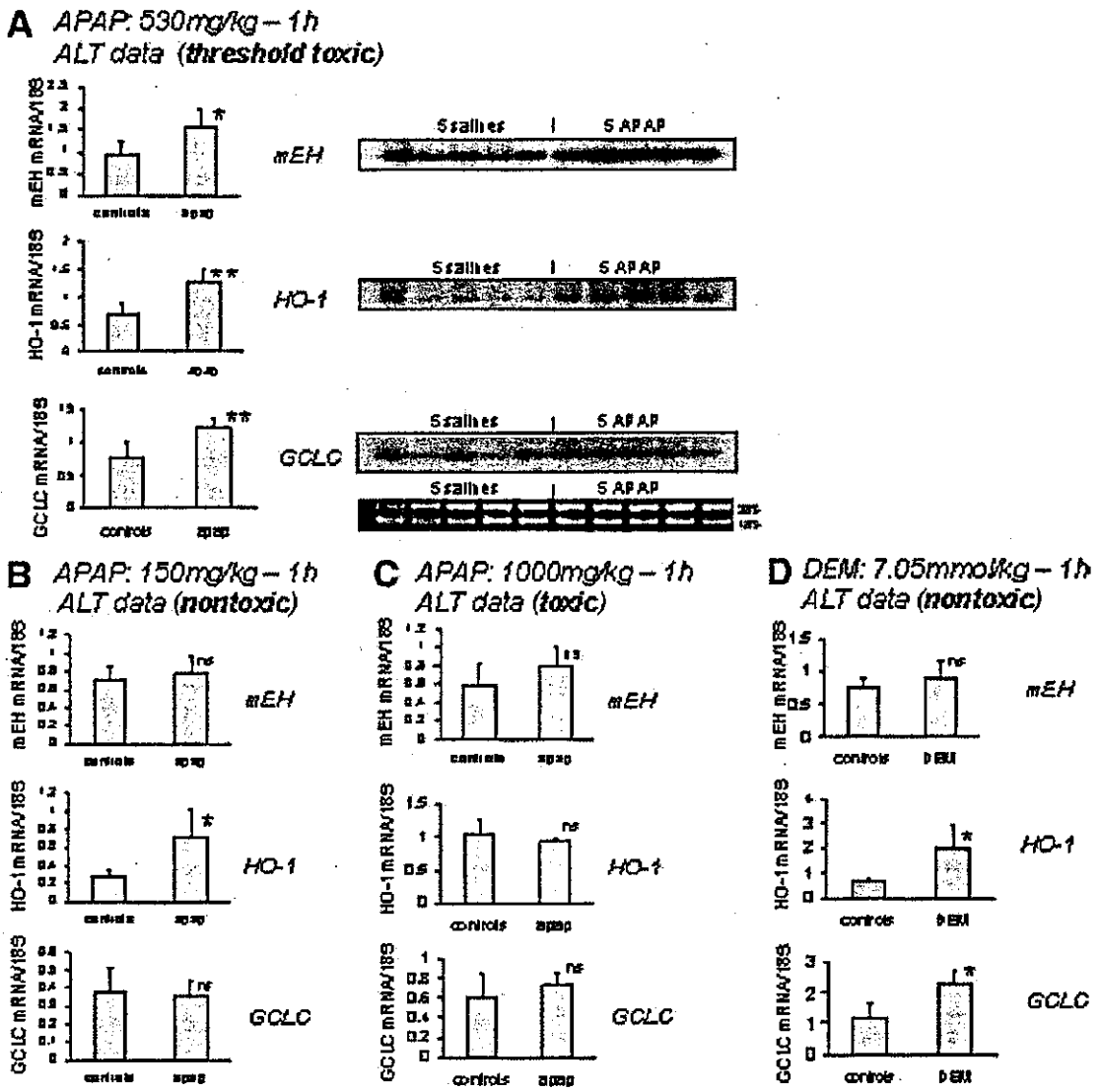

Fig. 5. Translocation of Nrf2 to the nucleus is functionally relevant as assessed by Northern blotting of Nrf2-dependent genes. Acetaminophen, or saline vehicle alone, and diethyl maleate (DEM), with time-matched controls, were administered IP to CD-1 mice (n = 5). After 60 minutes, animals were killed and the liver was removed and washed. Whole liver RNA was extracted and analyzed using Northern blotting (25 μg of total RNA from each animal), employing gene-specific probes corresponding to mouse mEH, HO-1, and GCLC mRNA sequences. In all cases,values are the means ± SD. For all data, values are standardized against 18S ribosomal RNA. Statistical significance was assigned relative to untreated control animals as defined in Materials and Methods. *$P < .05$; **$P < .01$; ns, not significant.

at the 530 mg/kg dose, which is a threshold dose for overt liver damage. Interestingly, none of the 3 Nrf2-regulated genes was induced at the highest (1000 mg/kg) dose despite the marked Nrf2 nuclear translocation occurring at this dose. Presumably, the level of toxicity associated with this dose results in such widespread cellular malfunctioning that the machinery involved in gene transcription and mRNA synthesis is itself impaired. In fact, cell death caused by acetaminophen may indicate that the toxic insult has overwhelmed repair mechanisms, such as the Nrf2 response, either by causing irreparable damage to it, or by causing other damage too great for the protective responses to deal with effectively. Differential induction of the 3 target genes was also observed with the single, high (7 mmol/kg) but nontoxic, dose of DEM used in this study, at which HO-1 and GCLC were both significantly up-regulated while mEH was unchanged. Thus, it appears that certain genes are more sensitive than others to Nrf2 activation and are induced at lower Nrf2 nuclear levels. Alternatively, since Nrf2 acts as a heterodimer to

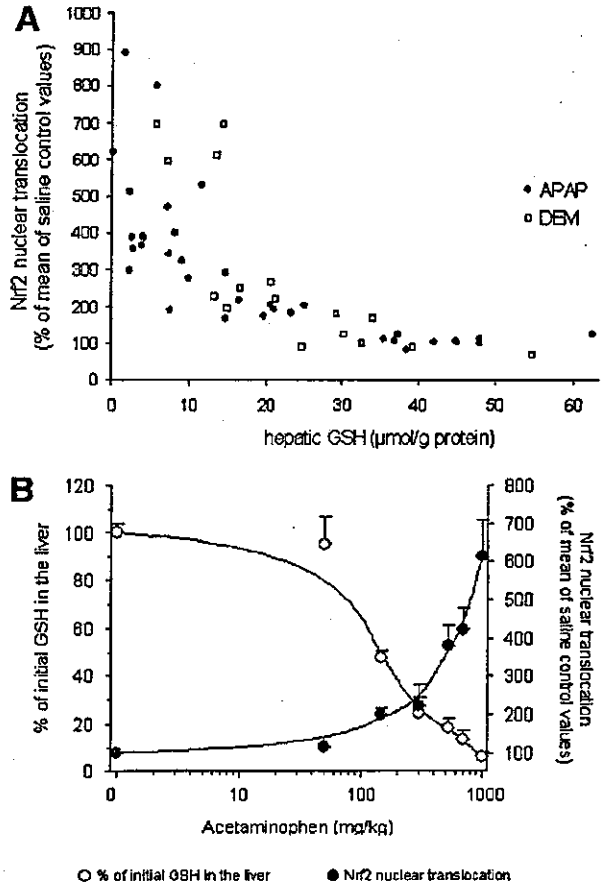

Fig. 6. Nrf2 nuclear translocation is associated with levels of hepatic glutathione (GSH). Acetaminophen, or saline vehicle alone, and diethyl maleate (DEM), with time-matched controls, were administered IP to CD-1 mice. After 60 minutes, animals were killed and the liver was removed and washed. (A) Hepatic GSH levels were determined and plotted against Nrf2 translocation. (B) GSH depletion and Nrf2 translocation were also expressed relative to the dose of acetaminophen. Data are expressed as the mean ± SD, where n = 5.

activate gene transcription, the differential induction of target genes observed may reflect their different preferences with respect to alternative dimerization partners. Precise characterization of the transcription factors recruited by variant forms of the ARE may be required in order to elucidate and define the hierarchical order of Nrf2 target gene transcription.

The linear response in Nrf2 translocation seen at the different doses of acetaminophen contrasts with the nonlinear response in Nrf2 when it is related to GSH. As GSH is depleted to approximately 30% of control levels, a modest increase in Nrf2 translocation is observed up to ≈200% of nuclear control levels (Figs. 6A and B). As GSH drops further, much more pronounced rises are seen in nuclear Nrf2. One could envisage a scenario in which depletion of GSH leads to increasing numbers of the reactive cysteine residues in the cytosolic Nrf2 inhibitor Keap1[22] becoming available to be oxidized or covalently modified (by the DEM molecule itself, or in the case of acetaminophen, by its reactive metabolite, NAPQI). In fact, the relationship we observe between Nrf2 translocation and GSH depletion is very similar to the relationship between hepatic covalent binding and GSH depletion upon administration of acetaminophen first observed by Mitchell et al.[44] This may be supportive of the notion that covalent binding (possibly of Keap1) via Michael addition is the precursor to Nrf2 activation *in vivo*, although a large number of cellular proteins that are adducted by acetaminophen have been identified[45]; it is also possible that the modification of 1 or more of these may play a role in triggering Nrf2 activation or other protective responses. Recent evidence suggests that there are 4 highly reactive cysteines within Keap1.[46] These are located in the intervening region between the 2 protein-binding domains of Keap1; this increases the likelihood that they may be available to act as sensors. The modification of some or all of these residues would lead to steadily increasing numbers of Nrf2 molecules translocating to the nucleus. At a certain threshold, further oxidation/modification of Keap1 may lead to substantial loss of association with Nrf2, enabling a wide-scale nuclear translocation. Whether Keap1 thiol modification occurs directly, possibly through Michael addition, or indirectly through preceding activation of upstream enzymes, is still unresolved. Recent investigations of the induction of GCLC by indomethacin and related indole compounds point to a role for NADPH (MTHFR; 5,10-methylenetetrahydrofolate reductase) oxidase in Keap1 thiol oxidation, through generation of the superoxide anion.[47] Although the universality of this mechanism needs to be clarified, formation of reactive oxygen species, including superoxide, has previously been postulated to be a consequence of acetaminophen metabolism,[32] and this may represent a further mechanism for Nrf2 activation. Evidence for a physiologically based mechanism for Nrf2 activation via covalent modification through Michael addition has recently emerged through studies on the prostaglandin J2 family of anti-inflammatory mediators.[48] These cyclopentenone compounds are dehydration products of prostaglandin D2, and as such contain the α,β-unsaturated ketone motif characteristic of Michael acceptors. Several of their properties, such as induction of glutathione S-transferases, are consistent with an interaction with the Nrf2 system, and it has recently been shown that they are indeed capable of the covalent modification of the Keap1 protein.[49,50] It is our intention to explore the possibility of direct modification of Keap1 by NAPQI